



**HAL**  
open science

## **New material of *Diacodexis* (Mammalia, Artiodactyla) from the early Eocene of Southern Europe**

Myriam Boivin, Maeva Orliac, Miguel Antunes Telles, Marc Godinot, Yves Laurent, Bernard Marandat, Dominique Vidalenc, Rodolphe Tabuce

► **To cite this version:**

Myriam Boivin, Maeva Orliac, Miguel Antunes Telles, Marc Godinot, Yves Laurent, et al.. New material of *Diacodexis* (Mammalia, Artiodactyla) from the early Eocene of Southern Europe. *Geobios*, 2018, 51 (4), pp.285-306. 10.1016/j.geobios.2018.06.003 . hal-03052875

**HAL Id: hal-03052875**

**<https://hal.science/hal-03052875>**

Submitted on 10 Dec 2020

**HAL** is a multi-disciplinary open access archive for the deposit and dissemination of scientific research documents, whether they are published or not. The documents may come from teaching and research institutions in France or abroad, or from public or private research centers.

L'archive ouverte pluridisciplinaire **HAL**, est destinée au dépôt et à la diffusion de documents scientifiques de niveau recherche, publiés ou non, émanant des établissements d'enseignement et de recherche français ou étrangers, des laboratoires publics ou privés.

1 **New material of *Diacodexis* (Mammalia, Artiodactyla) from the early**  
2 **Eocene of Southern Europe**

3

4 Boivin Myriam <sup>a</sup>, Orliac Maëva J. <sup>a,\*</sup>, Antunes Telles Miguel <sup>b</sup>, Godinot Marc <sup>c</sup>, Laurent  
5 Yves <sup>d,e</sup>, Marandat Bernard <sup>a</sup>, Vidalenc Dominique <sup>f</sup>, Tabuce Rodolphe <sup>a</sup>

6

7 <sup>a</sup> Institut des Sciences de l'Évolution de Montpellier, c.c. 064, Université de Montpellier,  
8 CNRS, IRD, EPHE, place Eugène Bataillon, F-34095 Montpellier Cedex 05, France

9

10 <sup>b</sup> Academia das Ciencias de Lisboa, 19 Rua da Academia das Ciências, 1249-122 Lisbon,  
11 Portugal

12

13 <sup>c</sup> EPHE, PSL, et Sorbonne Universités - CR2P - MNHN, CNRS, UPMC-Paris 6

14

15 <sup>d</sup> Muséum d'Histoire Naturelle de Toulouse, 35 allée Jules Guesde, F-31000 Toulouse, France

16

17 <sup>e</sup> Association Paléontologique du Sud-Ouest, 13 chemin des Telles, F-31360 Roquefort-sur-  
18 Garonne, France

19

20 <sup>f</sup> 103 avenue F. Mitterrand, 31800, St Gaudens, France

21

22 \* Corresponding author. E-mail address: [maeva.orliac@umontpellier.fr](mailto:maeva.orliac@umontpellier.fr) (M.J. Orliac).

23

24

25 **Abstract**

26 Diacodexidae are the first representatives of Artiodactyla in the fossil record. Their first  
27 occurrence is at the very base of the Ypresian (earliest Eocene, 56.0 Ma) with the genus  
28 *Diacodexis*. *Diacodexis* is a well-diversified genus during the early Eocene in Europe,  
29 especially during the MP7-MP8+9 interval. However, most of European species are  
30 documented by scarce material, retrieved from single localities. In this work, we describe new  
31 *Diacodexis* material from ~MP7 and ~MP8+9 localities of Southern Europe including  
32 material of *D. antunesi* from Silveirinha, considered as the most primitive European  
33 *Diacodexis*, and material from three localities from Southern France (Fordonnes, Palette, and  
34 La Borie). The new material documents *Diacodexis* premolar morphology and deciduous  
35 dentition which bear potentially important phylogenetic information, as well as astragali,  
36 including a specimen from Silveirinha that constitutes the earliest occurrence of an astragalus  
37 of the genus *Diacodexis* in the European fossil record. Investigation of the enamel  
38 microstructure reveals that early European species had a simple enamel pattern with one-  
39 layered Schmelzmuster composed of ‘basic’ radial enamel only, instead of the two-layered  
40 Schmelzmuster (thin radial enamel + thick layer of Hunter-Schreger bands) observed on  
41 North American species and so far considered to represent the primitive condition within  
42 Artiodactyla. In accordance with previous studies, our observations highlight that *Diacodexis*  
43 *gigasei* from Belgium is morphologically closer to the North American species *D. ilicis* than  
44 to *D. antunesi* from Portugal. The latter species, together with *D. aff. antunesi* from Fordones,  
45 appears to be morphologically closer to the Asiatic taxa *D. indicus* and *D. pakistanensis*.  
46 Finally, we found numerous similarities between *D. cf. gigasei* from Palette and *D. gigasei*, a  
47 result that challenges the intra-European provincialism that characterizes the earliest  
48 Ypresian. *Diacodexis gigasei* could be one of the rare species in common between  
49 northwestern and southwestern bioprovinces.

50

51 *Keywords:*

52 Diacodexidae

53 Ypresian

54 Enamel microstructure

55 Deciduous dentition

56 Astragalus

57

58

59 **1. Introduction**

60 Diacodexeid artiodactyls are the first representatives of even toed hoofed mammals in  
61 the fossil record (Rose, 1982, 2006; Theodor et al., 2007). Their first occurrence is found at  
62 the very base of the Ypresian (earliest Eocene, 56.0 million years ago) with the genus  
63 *Diacodexis* Cope, 1882. Based on this early occurrence in the fossil record and on their very  
64 simple tribosphenic molar pattern, Diacodexidae have been regarded as primitive among  
65 Artiodactyla (Cope, 1882; Romer, 1966; Van Valen, 1971; Godinot, 1981; Theodor et al.,  
66 2007). Formal phylogenetic analyses show *Diacodexis* as the first offshoot of the order  
67 (Geisler and Theodor, 2009) or close to the differentiation of crown artiodactyl groups  
68 (Gentry and Hooker, 1988; Geisler, 2001; Orliac and Ducrocq, 2012; Gatesy et al., 2012).

69 Together with other modern groups of mammals such as primates or perissodactyls,  
70 *Diacodexis* makes its first appearance in the fossil record during the Mammalian Dispersal  
71 Event (MDE), which coincides with the global climate warming of the Paleocene Eocene  
72 Thermal Maximum (or PETM) characterized by a global negative carbon isotope excursion  
73 (CIE) (Magioncalda et al., 2004; Gingerich, 2006). Species of *Diacodexis* have been reported  
74 from Eocene fossil localities on all continents of the Northern hemisphere, and dental, cranial  
75 and postcranial features of the genus are now well documented (e.g., Guthrie, 1971; Godinot,  
76 1981; Russell et al., 1983; Sigogneau-Russell and Russell, 1983; Sudre et al., 1983;  
77 Thewissen et al., 1983; Kumar and Jolly, 1986; Gingerich, 1989; Smith et al. 1996; Bajpai et  
78 al., 2005; Kumar et al., 2010; Orliac and Gilissen, 2012; Orliac and O’Leary, 2014).

79 *Diacodexis* is known from Asia, Europe, and North America, three places that have been  
80 alternatively proposed as center of origin of the genus (Thewissen et al., 1983; Krishtalka and  
81 Stucky, 1985; Smith et al., 1996). Europe and North America have housed, among others, the  
82 oldest *Diacodexis* (earliest Eocene) whereas the first occurrence of the genus in Asia is a little  
83 more recent (early Eocene; Kumar et al., 2010). The oldest North American species is *D.*

84 *ilicis* from Wasatchian-*Meniscotherium* (Wa-M) and Wasatchian-0 (Wa-0) biozones of the  
85 Wasatchian NALMA (North American Land Mammal Age) (Gingerich, 1989; Rose et al.,  
86 2012:92); Wa-M and Wa-0 faunas are, respectively, coincident with the maximum of the  
87 CIE and the main body of the PETM (Bowen et al., 2014).

88 In Europe, the first occurrence of *Diacodexis* also coincides with the onset of the  
89 PETM with *D. gigasei* from Dormaal (MP7 Reference Level) and Erquelinnes, Belgium  
90 (Smith et al., 1996; Smith et al., 2006; Missiaen et al., 2013) (Fig. 1). Other MP7 species are  
91 *D. antunesi* from Silveirinha, Portugal (Estravis and Russell, 1989), *Diacodexis* sp. from Le  
92 Quesnoy, France (Nel et al., 1999), *D. morrissi* from Abbey Wood, UK (Hooker, 2010),  
93 *Diacodexis* sp. from Kyson, UK (Sudre et al., 1983), *D. gazini* from Rians, France (Godinot,  
94 1981), and *Diacodexis* cf. *gazini* from Fordones, France (Marandat, 1991). Among these  
95 species, Estravis and Russell (1989) and Theodor et al. (2007) considered *D. antunesi* as the  
96 oldest, most primitive European *Diacodexis*. Later in the early Eocene, *Diacodexis* is known  
97 by two species: *D. corsaensis* from the MP8+9 locality of Corsà 0, Spain (Checa Soler, 2004)  
98 and *D. varleti* from several localities from the Paris Basin such as Condé-en-Brie, Mutigny,  
99 Avenay (MP8+9 Reference Level), and Pourcy (either MP7 or MP8+9) (Sudre et al., 1983)  
100 (Fig. 1). A closely related species, named *D. cf. varleti* was described from several MP 10  
101 localities also from the Paris Basin (Saint-Agnan, Cuis, Mancy, Prémontré, and Grauves)  
102 (Sudre et al., 1983; Sudre and Erfurt, 1996). The latest occurrence of *Diacodexis* cf. *varleti*  
103 dates from the “untere Unterkohle” (MP11) of the Geiseltal, Germany (Erfurt and Sudre,  
104 1996) (Fig. 1). Finally, several *Diacodexis* sp. indet. were mentioned from numerous  
105 localities from Spain, correlated with MP10 (Sudre et al., 1983; Antunes et al., 1997)

106 *Diacodexis* is therefore a well-diversified genus during the early Eocene in Europe,  
107 especially during the MP7-MP8+9 interval. However, most of European *Diacodexis* species  
108 are documented by scarce material, retrieved from a single locality. The scarcity of the

109 material often prevents comparing the same dental loci from two localities. Indeed, some  
110 localities yielded upper dentition only, while others yielded lower dentition. Besides, the lack  
111 of complete tooth rows makes dental association tricky. Finally, the scarcity of the  
112 documented material makes it difficult to apprehend the potential intraspecific variability that  
113 exists within *Diacodexis* species.

114 Here, we describe new material from ~MP7 and ~MP8+9 localities of Southern  
115 Europe that greatly increases our knowledge of European *Diacodexis* species. The new  
116 material comes from Portugal (Silveirinha), and Southern France (Fordones, Palette, and La  
117 Borie) and notably includes a mandible with p3-m3 and an upper cheek tooth row with P3-  
118 M3, which represents the most complete *Diacodexis* remains in Europe to date. The new  
119 material described also documents *Diacodexis* premolar morphology and deciduous dentition  
120 which bear potentially important phylogenetic information, as well as one astragalus from  
121 Silveirinha that constitutes the earliest mention of an astragalus of the genus *Diacodexis* in the  
122 European fossil record. The enamel microstructure of *Diacodexis* species from Silveirinha  
123 and Fordones is also investigated. These new data about European early *Diacodexis* species  
124 call into questions features considered as primitive within Artiodactyla, and allow discussion  
125 of the distribution and palaeobiogeographic relationships between Northern and Southern  
126 Europe near MP7.

127

## 128 **2. Material and methods**

### 129 *2.1. Material*

#### 130 *2.1.1. New material*

131 The material studied here comes from four localities, one is situated in Portugal  
132 (Silveirinha), the others in Southern France (Fordones, Palette, and La Borie) (Fig. 1).  
133 Silveirinha, Palette, and La Borie are well-known for having yielded rich mammalian faunas,

134 the most diversified ones for the early-middle Ypresian period of Southern Europe (e.g.,  
135 Antunes and Russell, 1981; Antunes et al., 1987; Estravis, 2000; Tabuce et al., 2006, 2009,  
136 2011 for Silveirinha; Godinot, 1984; Godinot et al., 1987; Solé et al., 2017 for Palette; and  
137 Laurent et al., 2010; Robinet et al., 2015; Solé et al., 2014 for La Borie). According to the  
138 Southern Europe biochronological sequence proposed recently for the beginning of the  
139 Eocene (Marandat et al., 2012), Silveirinha would be the oldest Southern European site  
140 referred to the MP7 level and Fordones and Palette –also referred to the MP7– would be co-  
141 eval and slightly younger than Silveirinha. Interestingly, Fordones and Palette are considered  
142 equivalent in age with another Southern French locality (Le Clot); the latter being estimated 1  
143 myr younger than the MP7 reference Dormaal locality (Yans et al., 2014). Finally, as for the  
144 locality of La Borie, Laurent et al. (2010) argued for a MP8+9 age. The mandible PAT 159  
145 from Palette was scanned at the CT-Scan facility of the Montpellier University with a  
146 resolution of 35 µm and 3D models representing its external surface and a virtual restoration  
147 of its ascending ramus are available on MorphoMuseuM (Orliac et al., in press, Models ID:  
148 M3#315\_ UMPAT159, M3#317\_ UMPAT159).

149

### 150 2.1.2. Comparison material

151 Comparisons are performed with *Diacodexis* species from Europe, Asia and North  
152 America. Observation of the European species are based on *D. antunesi* Estravis and Russell,  
153 1989 from Silveirinha, Portugal (direct observation of new material and on casts of the  
154 material figured by Estravis and Russell, 1989); *D. gigasei* Smith, Smith and Sudre, 1996  
155 from Dormaal, Belgium (direct observation on casts of the material); *D. morrissi* Hooker, 2010  
156 from Abbey Wood, England (observation from Hooker 2010: fig. 47 and direct observation  
157 on casts of M15141); *D. varleti* Sudre, Russell, Louis and Savage, 1983 from Condé-en-Brie,  
158 France (direct observation of the original material stored at the MNHN); *D. gazini* Godinot,



159 1981 from Rians, France (direct observation of the original material stored at the MNHN); *D.*  
160 *corsaensis* Checa Soler, 2004 from Corsà 0 (observation from Checa Soler, 2004: fig. 2).  
161 Observations of the Asian species are based on *Diacodexis pakistanensis* Thewissen et al.,  
162 1983 (= *Gujaratia pakistanensis*, see Kumar et al. 2010 p.1249) (known from several  
163 localities in India and Pakistan); *D. indicus* (Bajpai et al., 2005) (Vastan, India), *D. parvus*  
164 Kumar et al., 2010 (Vastan, India), and *Diacodexis* sp. from Andarak 2, Kyrgyzstan (based on  
165 Thewissen et al., 1983; Kumar et al., 2010; and Averianov, 1996 respectively). Finally,  
166 observations of the North American species *D. ilicis* Gingerich, 1989 (Bighorn Basin,  
167 Wyoming, USA) and *D. secans primus* Krishtalka and Stucky, 1985 (Bighorn and Powder  
168 River Basin, Wyoming and Four Mile area, Colorado, USA) are based on Gingerich (1989)  
169 and Rose et al. (2012), and Krishtalka and Stucky (1985) respectively.

170

## 171 2.2. Methods

### 172 2.2.1. Enamel microstructure

173 We studied the enamel microstructure of two *Diacodexis* specimens: one m2 from  
174 Silveirhina (SNC 3) and one fragmentary upper molar from Fordones (FDN 254). Sample  
175 preparation followed the protocol of Tabuce *et al.* (2007a). Casts of the specimens were made  
176 prior to preparation for enamel microstructure study. All specimens were embedded in epoxy  
177 resin and sectioned horizontally and tangentially. We subsequently performed 37 %  
178 phosphoric acid etching of the samples for 30 seconds to make the microstructural details  
179 visible. After rinsing with distilled water and drying, the samples were coated with conductive  
180 material (gold-palladium). They were observed and studied with two different scanning  
181 electron microscopes (SEM): HITACHI S4000 and S4800 (x250 to x500). Several parameters  
182 were evaluated in the description of enamel microstructure. Enamel thickness was measured  
183 perpendicularly to the Enamel-Dentine Junction (EDJ), and corresponds to the distance

184 between that plane and the Enamel Outer Surface (EOS). The orientation of the interprismatic  
185 matrix (IPM) is the angle between crystallites of the IPM and those of prisms. Each measure  
186 has been reproduced ten times.

187

### 188 2.2.2. *Abbreviations for institutions and dental nomenclature followed*

189 **Institutions:** CEPUNL, Centro de Estratigrafia e Paleobiologia da Universidade Nova  
190 de Lisboa; MHNT, Muséum d'Histoire Naturelle de Toulouse, Toulouse, France; MNHN,  
191 Muséum National d'Histoire Naturelle, Paris, France; UCMP, University of California  
192 Museum of Paleontology, Berkeley, USA; UM, Université de Montpellier, Montpellier,  
193 France.

194 The dental nomenclature mainly follows Boisserie et al. (2009) and Orliac and  
195 Ducrocq (2012).

196

## 197 3. Systematic paleontology

198

199 Order Artiodactyla Owen, 1848

200 Superfamily Dichobunoidea Gill, 1872

201 Family Diacodexidae Gazin, 1955

202 Genus *Diacodexis* Cope, 1882

203

### 204 3.1. *New material from the locality of Silveirinha Pequena, Baixo Mondego, Portugal*

205 The first mention of *Diacodexis* remains from the early Eocene locality of Silveirinha  
206 was made in the faunal list of the locality provided by Antunes and Russell (1981: p. 1101) as  
207 *Diacodexis* cf. *gazini*. Estravis and Russell (1989) subsequently revised the material and  
208 erected a new species, *Diacodexis antunesi* Estravis and Russell, 1989. In the latter work,

209 abundant dental remains of *D. antunesi* are described, documenting upper and lower molars,  
210 as well as dP4 and p2 or p3 of the species. Part of this *Diacodexis* material is also described  
211 and figured in the PhD thesis of Estravis (1992: p. 182-196). Additional material described  
212 here comes from field campaigns conducted in Silveirinha in the past 20 years.

213

214 *Diacodexis antunesi* Estravis and Russell, 1989

215 Fig. 2

216 **Synonymy:** 1981. *D. cf. gazini* - Antunes and Russell, p. 1101.

217 **Holotype:** r. m2 SV3 338 (coll. CEPUNL, in Estravis and Russell, 1989: pl. 1, fig. 2).

218 **Material** (coll. CEPUNL): in addition to that published by Estravis and Russell (1989) - SNC

219 64, dp2 or dp3 (left); SNC 386, p2 or p3 (left); SNC 74, m1-2 (right); SNC 6, m1 (right);

220 SNC 93, m1 (right); SNC 3, m2 (right); SNC 17, m3 (left); SNC 59, m3 (left); SNC 63, m3

221 (right); SNC 65, m3 (left); SNC 58, P3 (right); SNC 33, P4 (right); SNC 311, P4 (right); SNC

222 405, P4 (right); SNC 13, dP4 (left); SNC 49, M1 (right); SNC 339, M1 (right); SNC 20, M2

223 (right); SNC 25, M2 (right); SNC 36, M2 (right); SNC 55, M2 (left); SNC 95, M3 (right);

224 SNC 18, M3 (right); SNC 262, M3 (right); SNC 687, astragalus (right).

225 **Type locality and horizon:** Silveirinha Pequena, Baixo Mondego, Portugal; Silveirinha

226 Formation, Rio Mondego Member, early Eocene, ~MP7.

227 **Original diagnosis:** see Estravis and Russell (1989 : p. 31).

228 **Emended diagnosis:** very small species of *Diacodexis* with high and sharp cusps and

229 cuspids; long and well-marked crests; lower molars with central and low cristid obliqua;

230 hypoconulid small and close to entoconid on m1-2; short or absent labial cingulid; P3 with

231 small lingual lobe; P4 with strong preprotocristid, connected to the antero-labial corner of the

232 tooth, labial margin without ectoflexus; M1-2 with large parastyle protruding anteriorly;

233 lingual lobe of M1-2 clearly slenderer antero-posteriorly than the labial margin of the crown;

234 M3 triangular in shape compared to M2.

235 **Measurements:** Tables 1-2.

236 **Description:**

237 Lower dentition. Two lower premolars (SNC 64 and SNC 386) have been identified in  
238 addition to the deciduous premolar published by Estravis and Russell (1989: pl. 2.7) (Fig.  
239 2(A-D)). Both specimens present a low crown. The paraconid is lingually located and distinct  
240 from the preprotocristid. The hypoconid is separated from the postprotocristid by a small  
241 groove; in labial and lingual views, the hypoconid lies below the level of the paraconid. Based  
242 on the very small enamel thickness and on its low, labio-lingually narrow crown, SNC 64 is  
243 referred to as dp2 or a dp3. SNC 386 has a thicker enamel and a wider protoconid than SNC  
244 64 and rather documents permanent dentition, p2 or p3.

245 The new sample includes nine lower molars of *D. antunesi*. As noted by Estravis and  
246 Russell (1989), m1 has a large paraconid separated from the metaconid whereas this cuspid is  
247 clearly smaller on m2 (Fig. 2(M)). This character, together with the size of the tooth, allows  
248 for the m1-2 distinction. The trigonid becomes wider and the entoconid increases in both  
249 width and height from m1 to m3. The lower molars of *D. antunesi* present a trigonid with  
250 high and pointed cusps. Protoconid and metaconid are of sub-equal height, edges of the  
251 trigonid are defined by the preprotocristid and postprotocristid labially, by the  
252 postmetacristid, premetacristid, postparacristid lingually, and by the preparacristid anteriorly.  
253 The basin of the trigonid is deep; an endometafossid is observed on unworn teeth, as well as a  
254 clear postmetafossid. The basin of the talonid is delimited labially by a low cristid obliqua  
255 (=prehypocristid). Lingually, the ectoentocristid is short and low and connects a very slight  
256 postectometacristid. The postectometacristid is variably absent or very slight in the new  
257 sample, a character also observed on the material published by Estravis and Russell (1989).  
258 The anterior end of the low cristid obliqua occupies a central position on all lower molars of

259 our sample: it reaches anteriorly the level of the trigonid notch. On m1-2, the hypoconulid is  
260 connected to the entoconid, to the hypoconid and to a long posterior cingulid by high cristids.  
261 The hypoconulid is closely apposed to the entoconid. The labial cingulid is short or absent on  
262 m1-2. Despite important variations concerning the posterior lobe of m3, in all specimens, the  
263 hypoconulid is clearly distinct from the talonid on m3 and a deep groove separates the  
264 hypoconulid from the entoconid. A small accessory cusp, labial to the hypoconulid, can occur  
265 (Fig. 2(J)).

266 Upper dentition. The new sample includes five upper premolars, including a decidual  
267 one. Two new premolar loci are documented here in addition to the dP4 already described by  
268 Estravis and Russell (1989). SNC 58 is broken in its lingual part but its shape indicates a P3  
269 (Fig. 2(S)). Its parastyle is reduced and embedded in the anterior cingulum. The posterior part  
270 of the tooth is occupied by a large metastyle. The lingual portion of the tooth is broken and  
271 the extension of the lingual lobe cannot be assessed. The P4 is subtriangular in occlusal view  
272 (Fig. 2(R)). The protocone is located slightly anterior to the paracone. The paracone is  
273 considerably larger and higher than the protocone and bears three cristae, a preparacrista and a  
274 postparacrista connected to a large parastyle and a smaller metastyle respectively, plus a clear  
275 and sharp endoparacrista, located low in the valley between the paracone and protocone. On  
276 both P4 specimens (SNC 405 and SNC 311), the endoparacrista connects to a very small  
277 endoprotocrista. The protocone shows a sharp preprotocrista merging anteriorly with the  
278 anterior cingulum; there is no postprotocrista. The parastyle is large especially on SNC 311  
279 illustrated in Figure 2(R). There is no ectoflexus. The lingual, anterior and posterior cingula  
280 are continuous. The dP4 (SNC 13, Fig. 2(T)) is morphologically very close to that described  
281 by Estravis and Russell (1989: pl. 2.5). The tooth is posterolabially elongated, especially in its  
282 disto-labial corner. This character, together with its small width (Table 1), indicate that it is a  
283 deciduous tooth. DP4 morphology is very close to that of permanent upper molars. The

284 protocone is big and low, and bears two thick cristae, the preprotocrista and the  
285 postprotocrista. They project toward the protoconule and the metaconule respectively but are  
286 separated from the latter by grooves. The metaconule and the protoconule are small and  
287 pointed. The metaconule bears three cristae: small pre and endometacristule, and a longer  
288 postmetacristule, which joins the metastyle at the disto-labial corner of the tooth. The  
289 endometacristule connects a small endometacrista, at the base of the metacone. Likewise, the  
290 protoconule bears a preprotocristule which joins the parastyle; yet, the endoprotocristule is  
291 lacking.

292         The M1-2 have a rather characteristic morphology (Fig. 2(P-Q)). The cusps are sharp  
293 and high, with well-marked cristae. The parastyle is large and projects/protrudes on the  
294 anterior edge of the tooth. A pericone is sometimes present (SNC 20, 55 and 74), a small  
295 hypocone is observed on some specimens (SNC 25 and 74). The preparacrista and  
296 postmetacrista are sharp, often both on the same plane as the centrocrista. The paraconule and  
297 the metaconule both present pre-, endo- and postcristae. The endopara and endometacristules  
298 connect the endopara and endometacrista respectively. The anterior and posterior cingula are  
299 long, thick, but never connect lingually. In occlusal view, the posterior edge of the crown  
300 shows an internal angle at the point where the postmetacristule joins the postero-labial corner  
301 of the tooth. The labial edge is straight except on the M2 SNC 20. The M1 SNC 49 differs  
302 from the other molars collected at Silveirinha by a weak parastyle, weak cingula, and a round  
303 shape at the base of the metacone and paracone. However, these observations could be due to  
304 a particular taphonomic history. Indeed, the enamel is thin or absent on the labial part of the  
305 tooth. The latter could have been digested by a predator. The M3s show a triangular outline.  
306 The three M3 of the new sample (SNC 18, SNC 75, and SNC 262) have a more rounded  
307 lingual outline than the specimen figured by Estravis and Russell (1989: pl. 2.1; SV3 126).  
308 M3s show a crest pattern similar to that of M1-2.

309           Observed variation on dental material. The dental material shows some morphological  
310 variability. Variation on lower molars is observed on the length of the cingulids, the presence  
311 of the labial cingulid, and the connections of the posterior cristids of the talonid of the m3  
312 (Estravis and Russell, 1989). Among the molar sample, variation on the paraconid size is also  
313 observed with the m3 SNC 17, which has a smaller paraconid. We interpret these differences  
314 as part of the plausible intraspecific variation. Indeed, the case of one specimen with a  
315 reduced paraconid within a *Diacodexis* sample has already been reported from other localities  
316 (Sudre et al., 1983; Kumar et al., 2010). All the material from Silveirinha is referred here to  
317 the species *D. antunesi*.

318           Enamel microstructure. The lower molar SNC 3 presents a ‘basic’ radial enamel on the  
319 whole enamel thickness (Fig. 3). Its thickness varies from 37 to 152  $\mu\text{m}$ , its average is 91  $\mu\text{m}$ .  
320 There is no synchronous prism undulation. The prisms have an average diameter of 4  $\mu\text{m}$ .  
321 Prisms rise from the EDJ at an angle of  $64^\circ$  and reach EOS with an angle of  $78^\circ$ . The IPM  
322 forms a closed coat. The IPM crystallites are at an angle of  $27^\circ$  with those of prisms. The  
323 outer aprismatic part represents on average 4.5% of the enamel thickness.

324           Astragalus. In addition to the new dental material, one astragalus was also found at  
325 Silveirinha and constitutes the first mention of postcranial remains attributed to *Diacodexis*  
326 *antunesi*. The astragalus SNC 687 (Fig. 2(U-W), Table 2) is broken below the sustentacular  
327 facet and the distal trochlea is missing. The two crests of the tibial trochlea are separated by a  
328 deep groove. They are asymmetric, the lateral condyle being higher than the medial one.  
329 There is no fossa for the anterior process of the tibia. The fossa for the tibial malleolus is wide  
330 and deep. The fibular sulcus is well marked in posterior view. The sustentacular facet is long,  
331 ovoid and its long axis is directed slightly proximomedially. The sustentacular facet is only  
332 slightly convex laterally. The ectal facet, separated from the sustentacular facet by a wide  
333 sulcus tali, is shrunk in its central part but more extended in its upper half.

334 **Remarks:**

335 Comparison with MP7 and MP8+9 Southern European species. *Diacodexis antunesi*  
336 differs from most other species of the genus by its smaller size, especially for the lower  
337 molars (Figs. 4-5). Compared to *D. gazini* from the slightly more recent locality of Rians  
338 (Marandat et al., 2012), *D. antunesi* shows less massive upper and lower molars, with deeper  
339 labial notches in occlusal view between the trigonid and the talonid on lower molars and  
340 between the labial and lingual cusps on the upper molars. *D. antunesi* has smaller entoconid  
341 and hypoconid on lower molars (Fig. 6). On upper molars, the parastyle of *D. antunesi* is  
342 larger and protrudes anteriorly; on M1-2, the postmetacristule and preprotocristule are salient  
343 which confers to the crown an hourglass shape, something not observed on *D. gazini* which  
344 crown is more rectangular; when present, the hypocone of *D. antunesi* is smaller than that of  
345 *D. gazini* on M1-2. *D. antunesi* seems to show a close morphology to the poorly illustrated *D.*  
346 *corsaensis* from the MP8+9 locality of Corsà 0, Spain (Checa Soler, 2004: fig. 2), represented  
347 by lower dentition only. All dental remains of *D. corsaensis* are of larger size than *D.*  
348 *antunesi* (Fig. 4).

349 Comparison with MP7 Northern European species. Lower molars of *D. antunesi* differ  
350 from those of *D. gigasei* from Dormaal (Belgium) in having a smaller paraconid (especially  
351 on m1), a lower cristid obliqua on m1-2, a hypoconulid on m1-2 situated closer to the  
352 entoconid. The fresh lower molars of *D. gigasei* show a distinct endohypocristid (Fig. 6). The  
353 upper molars of *D. antunesi* and *D. gigasei* are close morphologically, but the parastyle is  
354 bigger in *D. antunesi*. They are also close regarding M3 proportions (Fig. 5). The P4 of *D.*  
355 *gigasei* presents an ectoflexus that is not present in the specimens of *D. antunesi* (Fig. 7(K)).  
356 The first lower molar of *Diacodexis antunesi* differs from that of *D. morrisi* (from MP7 of  
357 England) by a narrower talonid, and a lower and more central cristid obliqua. The upper  
358 molars of *D. morrisi* are more rounded lingually, and present a smaller parastyle; the groove



359 intersecting the postprotocrista is deeper in *D. morrisi* (Fig. 7(G)). Despite a smaller size, *D.*  
360 *antunesi* is morphologically very close to *D. varleti*. Both species present a hypoconulid of  
361 m1-2 situated close to the entoconid, a protoconid almost as high as the metaconid on lower  
362 molars, hourglass-shaped upper M1-2 with salient postmetacristule. Morphological  
363 differences consist in a smaller parastyle of the upper molars less protruding anteriorly for *D.*  
364 *varleti*; M3s of the latter species also have a greater anteroposterior length (Fig. 5).

365 Comparison with Northern American species. *Diacodexis antunesi* differs from *D.*  
366 *ilicis* from the Wasatchian of North America in having more pointed cuspids/cusps. The lower  
367 molars of North American species have a paraconid located more lingually. In *D. antunesi*,  
368 the hypoconulid of m1-2 is situated closer to the entoconid. On upper premolars, the paracone  
369 of P3 of *D. antunesi* is larger than that of *D. ilicis* and it does not seem to present the  
370 accessory cusp on the postparacrista observed in *D. ilicis* (Rose et al., 2012: fig. 51.D). The  
371 protocone lobe of P3 seems to be less distinct in *D. antunesi* (broken on the only available  
372 specimen). The P4 of *D. antunesi* presents a straight posterior edge, whereas *D. ilicis* shows  
373 an anterior deflection of the lingual part of the crown. The upper molars of *D. antunesi* and *D.*  
374 *ilicis* are close morphologically with an angular lingual lobe, sharp and salient  
375 preprotocristule and postmetacristule, and a parastyle protruding anteriorly. Based on what is  
376 preserved of the astragalus, the sustentacular facet seems to be larger in *D. antunesi* than in *D.*  
377 *ilicis*.

378 Comparison with Asian species. *Diacodexis antunesi* differs from *D. indicus* in being  
379 smaller and in having a wider sulcus tali, a very long and posterolabially expanded  
380 postmetacrista on dP4, more transverse upper molars with stronger parastyle and metastyle,  
381 and more posteriorly deflected postprotocrista on M2; its lower molars have a less elevated  
382 and a more labial cristid obliqua and shorter and weaker anterior cingulids. *Diacodexis*  
383 *antunesi* similarly differs from *D. pakistanensis* by its transverse upper molars with strong

384 parastyle and metastyle; it further differs from this Asian species by a larger paraconid on  
385 lower molars. *Diacodexis antunesi* differs from *D. parvus* in having a metacone and paracone  
386 of similar size, an incomplete lingual cingulum, a more posterior orientation of the  
387 postprotocrista on M2, and an undivided ectal facet on the astragalus. *Diacodexis antunesi*  
388 differs from *Diacodexis* sp. from Andarak 2 by more transverse upper molars with anterior  
389 cingulum and sharp endoparacristule.

390

### 391 3.2. New material from the locality of Fordones, Aude, France.

392 Some specimens of *Diacodexis* from Fordones were described by Marandat (1991)  
393 and referred to *Diacodexis* cf. *gazini*. This material includes dp4, m1-2, and P2-3, but only the  
394 dp4 and the m1 were figured (Marandat, 1991: pl.4, figs. 10, 12, 14). We provide here  
395 additional views of these specimens and figure the loci that were not illustrated in Marandat  
396 (1991). Revision of the material referred to *Diacodexis* by Marandat (1991) revealed that the  
397 fragmentary m3 FDN 253 is not *Diacodexis* and rather belongs to a primate. Additional  
398 material from Fordones was collected in 2009. During screen washing, a P3-M3 series was  
399 retrieved in the same sieve and most probably belongs to the same individual, the bone of the  
400 maxilla was possibly not preserved during diagenesis and only teeth fossilized. Unfortunately,  
401 the M1 is missing.

402

### 403 *Diacodexis* aff. *antunesi*

404 Fig. 8

405 **Synonymy:** 1991. *Diacodexis* cf. *gazini* – Marandat, pl. 4, figs. 10, 12, 14.

406 **Material** (coll. UM): FDN 279, p2 or p3 (right); FDN 122, dp4 (left fragment); FDN 123,  
407 dp4 (left); FDN 124, m1 (left); FDN 255, m1 (right); FDN 125, m2 (right); FDN 252, P2  
408 (right); FDN 251, P3 (right); FDN 254, M (fragment); FDN 280, M (left fragment); P3-4 and

409 M2-3 FDN 283 (right).

410 **Locality and horizon:** Fordones, Aude, France; «Grès à nummulitidés» Formation, early  
411 Eocene, ~MP7.

412 **Measurements:** Table 3.

413 **Description:**

414 Lower dentition. One permanent lower premolar of *Diacodexis* is documented (FDN  
415 279) from Fordones (Fig. 8(D-F)). By its size and morphology, it either represents p2 or p3.  
416 Despite wear, a small paraconid is visible. The hypoconulid is central and distinct from the  
417 postparacristid. The dp4 (FDN 123) presents a protruding and deeply basined anterior lobe  
418 with a high paraconid. The paraconid lies in a central position and slightly extends lingually.  
419 The anterior basin is delimited by high and sharp cristids originating from the paraconid and  
420 joining the preprotocristid labially and the premetacristid lingually. The cristid joining the  
421 protoconid is worn and the lack of a primonid cannot be directly verified; however, there is no  
422 swelling of the cristid. The protoconid and metaconid are of equal size, and located on the  
423 same transversal plane; both bear postcristids. A small basin is present between the  
424 protoconid and metaconid, delimited by incipient endofossids. There is no clear endoproto-  
425 and endometa- cristids. The lingual cutting edge of dp4 is composed of high premetacristid,  
426 postectometacristid and ectoentocristid. The entoconid also bears a small endoentocristid and  
427 a sharp postentocristid. The latter is not connected to the posthypocristid. The cristid obliqua  
428 connects the base of the metaconid. There is no hypoconulid. Concerning the root pattern, the  
429 dp4 bears only two pillars, there is no trace of third labial pillar (see discussion). A  
430 fragmentary dp4 documenting the trigonid (FDN 122) shows the same morphology as FDN  
431 123.

432 The lower molars are documented by two m1 and one m2. All specimens are worn and  
433 the finest structures of the crest and groove pattern have been worn away. The specimens

434 show a long and thin anterior cingulid; the labial cingulid is absent. Compared to m1, the  
435 trigonid of m2 is more compressed due to the posterior position of the paraconid (appressed to  
436 the metaconid). On m1-2, the cristid obliqua joins the base of the protoconid (Fig. 8(G-L)).  
437 Marandat (1991) considered that the hypoconulid was absent and that the entoconid was  
438 connected to the posterior cingulid. However, these observations are related to the wear of the  
439 teeth, a small groove and the shape of the exposed dentine indicate that a small hypoconulid  
440 was indeed present. The apparent connection of the entoconid to the posterior cingulum is  
441 also due to wear. The talonid notch is deep and marked.

442 Upper dentition. The upper dentition of *D. aff. antunesi* is documented by two isolated  
443 premolars and by an upper tooth row comprising P3-4, M2-3 (FDN 283). The P2 (FDN 252)  
444 is slightly inflated in its posterolingual part, but its posterior-most portion is broken (Fig.  
445 8(Q)). There are sharp and high pre- and post- paracristae. A very small parastyle lies  
446 anteriorly to the preparacrista. The postparacrista and preparacrista are finely crenulated. The  
447 P3 is documented by two specimens (FDN 283, FDN 251). It has a triangular outline (Fig.  
448 8(P)) and three well separated roots, one anterior, one posterior and one supporting the lingual  
449 lobe. The paracone bears sharp and high pre- and post- paracristae. The parastyle is salient  
450 and distinct from the preparacrista. The postparacrista joins the posterior cingulum at the level  
451 of the metastyle. The lingual lobe is small and bears no protocone; a small basin is present,  
452 lined by a thin lingual cingulum. In both specimens, the lingual cingulum is continuous with  
453 the posterior one. The P4 shows a rather small protocone, which summit is more anterior than  
454 that of the paracone (Fig. 8(O)). The protocone bears a sharp preprotocrista joining the  
455 anterior cingulum, but no posterior crista. There is no endoprotocrista and no endoparacrista.  
456 The posterior cingulum is thick, long and joins a small metastyle on the posterolabial corner  
457 of the tooth. The cingulum is interrupted lingually at the protocone level. The labial cingulum  
458 is thin and continuous. There is no ectoflexus.

459 The M2 (FDN 283) has a trapezoidal outline (Fig. 8(N)). The labial edge is straight  
460 and the lingual lobe is antero-posteriorly wide. The anterior cingulum is long and ends  
461 lingually at the level of a small pericone whereas the posterior cingulum is less extensive but  
462 thicker with a small hypocone. The parastyle is small. Wear does not obscure the presence of  
463 the endoproto- and endometacristules. The M3 is triangular in shape. It exhibits a  
464 pronounced ectoflexus and the paracone is larger than the metacone (Fig. 8(M)). The  
465 protocone is smaller than on M2. The anterior cingulum joins lingually a small pericone. In  
466 the upper tooth row, the size of M3 is only slightly smaller than M2, whereas P4 is  
467 considerably smaller than the latter (Fig. 8(M-O)).

468 Enamel microstructure. The 'basic' radial enamel of the upper molar FDN 254 from  
469 Fordones has the same characteristics as that of *D. antunesi* (Fig. 3). It is slightly thinner (84  
470  $\mu\text{m}$ ) and the IPM cristallites are directed to  $33^\circ$  relative to the prism direction. Prisms rise  
471 from the EDJ at an angle of  $65^\circ$  and reach EOS with an angle of  $72^\circ$ . The aprismatic outer  
472 enamel layer is thicker than in *D. antunesi*: it represents on average 20% of total enamel  
473 thickness.

474 **Remarks:** *D. aff. antunesi* is morphologically very close to *D. antunesi* from the slightly  
475 older locality of Silveirinha, Portugal. The upper teeth are generally the same size: upper  
476 molars fall in the range of variation observed in *D. antunesi*, the P4 is slightly larger labio-  
477 lingually (Fig. 5). However, greater size difference is observed for m1-2, with specimens of  
478 *D. aff. antunesi* from Fordones larger than those of *D. antunesi* (Fig. 4). Compared to *D.*  
479 *antunesi*, m1-2 of *D. aff. antunesi* have a larger entoconid that widens the talonid part of the  
480 tooth. Both taxa show the same crest pattern and a hypoconulid closely linked to the  
481 entoconid, as well as subequal trigonid and talonid, separated by deep labial and lingual  
482 notches (Fig. 7(C)). Like *D. antunesi*, the P4 of *D. aff. antunesi* has no ectoflexus; however,  
483 the parastyle and the paracone are smaller and the endoparacristule is lacking in *D. aff.*

484 *antunesi*. The P3 of *D. aff. antunesi* differs from that of *D. antunesi* by a slenderer distal part  
485 with a weaker cingulum. Because of these differences and of the small number of remains  
486 available from Fordones, we decided to refer it to as *D. aff. antunesi*.

487 Marandat (1991) referred the *Diacodexis* remains from Fordones to *Diacodexis* cf.  
488 *gazini* based on dimensions of the lower molars slightly larger than *D. antunesi* and on  
489 characters he considered also present in *D. gazini*: lack of hypoconulid on lower molars,  
490 entoconid small and fused to the posterior cingulid, a paraconid close to the metaconid. Based  
491 on our new observations, the absence of hypoconulid in the lower molars of Fordones and in  
492 the specimens of *D. gazini* from Rians is due to wear: the hypoconulid has been worn away;  
493 the connection of the entoconid to the posterior cingulid and the proximity of the paraconid  
494 and metaconid are also characters related to the wear stage of the teeth. Compared to *D.*  
495 *gazini* from the more recent locality of Rians (Marandat et al., 2012), *D. aff. antunesi* from  
496 Fordones has less internal paraconid and metaconid and thinner cingulids on lower molars.  
497 Upper molars of *D. aff. antunesi* have more pointed cusps, the lingual lobe of M2 is  
498 proportionally wider in *D. gazini* due to massive cingula. The ectoflexus of upper molars is  
499 shallower in *D. gazini* (Fig. 7(C) vs (E)). Like *D. antunesi*, *D. aff. antunesi* is morphologically  
500 very close to *D. varleti* but shows smaller dimensions of upper and lower teeth. The M2  
501 specimen from Fordones is much smaller, but M3s of both species have the same labio-  
502 lingual diameter but they are much longer in *D. varleti* (Fig. 5). The dp4 of *D. varleti* (CB  
503 811) is also mentioned in the literature (Sudre 1983:295) but could not be found in the  
504 MNHN collections and is possibly lost. *D. aff. antunesi* from Fordones differs from other  
505 early Ypresian *Diacodexis* species for the same characters as those mentioned for *D. antunesi*.  
506 For additional comments on enamel microstructure and dp4 morphology and comparisons  
507 with other *Diacodexis* species, see discussion section.

508

509 3.3. *New material from the locality of Palette, Bouches-du-Rhône, France*

510 *Diacodexis* material from Palette was mentioned by Godinot et al. (1987) who  
511 tentatively referred one astragalus to cf. *Diacodexis*. The dental material of *Diacodexis* from  
512 Palette, identified and prepared in 2012, confirms the presence of this genus in this locality.

513  
514 *Diacodexis* cf. *gigasei*

515 Figs. 9-10

516 **Referred material** (coll. UM): PAT 159, dentary with p3-m3 and alveoli i1-p2 (left); PAT  
517 136, m1 (left); PAT 19, astragalus (left); PAT 168, astragalus (right).

518 **Locality and horizon:** Palette, Bouches-du-Rhône, France; at the top of the «Calcaires de  
519 Langesse», early Eocene, ~MP7.

520 **Measurements:** Tables 2, 4.

521 **Description:**

522 Dentary. PAT 159 consists in a left dentary preserving p3-m3 (Fig. 9). The anterior-  
523 most part of the mandible is preserved and the alveoli of i1-p2 are visible. The body of the  
524 mandible is free from deformation and complete except for a small portion of its ventral edge,  
525 broken under p4-m1. The posterior part of the mandible, including the angular apophysis, is  
526 missing. The ascending ramus is deformed: its height and width are diminished by fractures  
527 and medial sliding of the bone. The 3D model of the originally preserved state specimen as  
528 well as a 3D model showing a reconstruction of the ascending ramus based on the preserved  
529 fragments are available at MorphoMuseum.com (Orliac et al., in press; models ID: M3#315\_  
530 UMPAT159, M3#317\_ UMPAT159). PAT 159 constitutes the most complete specimen of  
531 European *Diacodexis* to date, and the longest tooth row documented for the same individual  
532 for European *Diacodexis* species. The body of the mandible is particularly slender and low,  
533 especially in the incisors and canine region, and slightly increases from the incisors to the

534 molars, but is of constant height between p3 and m2. The body of the mandible is particularly  
535 shallow at the level of p1 where it slopes downward (Fig. 9(A-B)). Three mental foramina are  
536 present on the labial surface: one below the p1, one below the posterior root of the p2, and  
537 one between the p3 and p4. The first mental foramen is the largest. The mandibular  
538 symphysis starts from the level of p2. Despite of breakage of the posterior part of the  
539 mandible, the coronoid apophysis is complete; it is slightly curved posteriorly and shows a  
540 wide plateau at its dorsal extremity. Its dorsal extension is weak: its height is similar to the  
541 height of the body of the mandible at the level of m3. This is, to our knowledge, the first  
542 documentation of a complete coronoid apophysis for *Diacodexis*, except the conceptual  
543 reconstruction provided by Russell et al. (1983: fig. 1) for *D. pakistanensis* in which the  
544 dorsal extremity was figured in dotted lines. The anterior part of the mandibular condyle is  
545 preserved, separated from the ascending ramus by a wide incisura. The condyle, which was  
546 small in size, was situated well above the tooth row. There is a large space between the root of  
547 the ascending ramus and the posterior part of m3. Based on the disposition of the alveoli on  
548 the anterior portion of the mandible, there were three short diastemata between p3 and p2,  
549 between p2 and p1, and between p1 and canine. The canine and the p1 are single-rooted, the  
550 p2 is double-rooted and its size was probably similar to that of the p3. The alveolus of p1 and  
551 that of the canine are similar in size. Judging from the size of their alveoli, the incisors of *D.*  
552 *cf. gigasei* were minute. Alveoli of i1-i2 are coalescent.

553 Lower tooth row. The p3 has a tiny paraconid connected to the protoconid via the  
554 preprotocristid. The postprotocristid joins the posterolingual cingulid but the hypoconid only  
555 consists in a bulge of the posterior cingulid. The p3 has no anterolabial cingulid. The p4 is  
556 wider than p3, longer, and has a more distinct paraconid and a rather larger hypoconid than  
557 p3. Compared to p3, a small anterolingual cingulid is present and the anterior and posterior  
558 basins are more elongate. Three posterior crests originate from the protoconid, a long



559 postprotocristid, and short endoprotocristid and postectoprotocristid. On p3-4, the  
560 preprotocristid is labial and is shifted lingually in its anteriormost portion to join the  
561 paraconid. The m1 is antero-posteriorly shorter than p3 and p4. The m2 is the widest molar  
562 labio-lingually and its length is clearly superior to that of m1 (Table 4). On m1-3, the talonid  
563 is larger than the trigonid; the cristids of the trigonid are close together and the trigonid basin  
564 is narrow. The paraconid is almost as high as the protoconid, which itself is small and close in  
565 size to the metaconid. The protoconid and the metaconid are about the same height. The  
566 paraconid is distinct from the metaconid on m1, these two cuspids being less separated on  
567 m2-3. In spite of wear, the endoprotofossid and endometafossid are present. The talonid notch  
568 is weak and the postectometacristid is absent on m1-3. The entoconid is located lingually and  
569 large but smaller than the hypoconid. The cristid obliqua is directed toward the metaconid on  
570 m1 and central on m2-3. The anterior cingulid is long and almost continuous with the labial  
571 cingulid on m2-3. The hypoconulid is linked to the entoconid, to the hypoconid and to the  
572 posterior cingulid except on m3 where it is separated from the labial cingulid by a groove.  
573 The posterior lobe of the m3 is massive and bears a large hypoconulid.

574 Astragalus. Two astragali retrieved in Palette are referred here to the species *D. cf.*  
575 *gigasei*. They are identical in terms of size and proportions. The proximolateral part of the  
576 tibial trochlea is missing on the astragalus PAT 168 whereas the astragalus PAT 19 is almost  
577 complete, with only the tibial trochlea lateral condyle and the distal calcaneal facet partly  
578 broken (Fig. 10(A-D)). The two trochlea of the astragalus PAT 19 have the same width. In  
579 both specimens, the groove of the tibial trochlea is wide and shallow, and the condyles are  
580 nearly symmetrical proximally. The fossa for the anterior process of the tibia is present on  
581 PAT 19 (corresponding part broken on PAT 168). On both specimens, the distal trochlea is  
582 robust and has a very prominent cuboid facet, which is especially pronounced on PAT 19.  
583 The fossa for the tibial malleolus is deep and the sustentacular facet is long and strongly

584 convex in lateral view. The surface where fits the calcaneo-navicular ligament is wide on both  
585 specimens. The ectal facet is shrunk in its center, and its upper part is round. The ectal facet is  
586 separated from the sustentacular facet by a narrow sulcus tali. Slight differences are observed  
587 between the two specimens: the neck of PAT 19 is narrower than that of PAT 168 (Fig. 10(A)  
588 vs (E)) and its lateral cavity is deeper.

589 **Remarks:**

590 Comparison with other known *Diacodexis* dentaries. Dentaries of *Diacodexis* figured  
591 in the literature are scarce and, to our knowledge, only available for *D. indicus* (Kumar et al.,  
592 2010: fig. 5E), *D. secans* (Krishtalka and Stucky, 1985), and *D. pakistanensis* (Russell et al.,  
593 1983: fig. 1; Thewissen et al., 1983). A decent fragment of the mandible of *D. ilicis* is also  
594 illustrated in Gingerich (1989). The morphology of the mandible remains undescribed for  
595 European taxa so far. The three diastemata observed in *D. cf. gigasei* (between p3 and p2,  
596 between p2 and p1, and between p1 and canine) are also present in *D. pakistanensis* as figured  
597 by Russell et al. (1983: fig. 1). The material illustrated by Thewissen et al. (1983: pl. 2) shows  
598 that variability occurs in that species and that the p3-p2 diastema can be present or absent  
599 (Thewissen et al., 1983: pl. 2.4 vs 5). Short diastemata between p2 and p1 and p1 and canine  
600 are also present in *D. indicus* (Kumar et al., 2010: fig. 5E) and *D. secans* (Krishtalka and  
601 Stucky, 1985). The p3-p2 diastema is also observed in *D. secans* (Krishtalka and Stucky,  
602 1985), but does not seem to be present on the specimen of *D. indicus* (Kumar et al., 2010: fig.  
603 5E). Compared to the specimen of *D. pakistanensis* figured by Thewissen et al. (1983: pl.  
604 2.4a), to *D. indicus* (Kumar et al., 2010: fig. 5G) and to *D. ilicis* (although most probably  
605 deformed, Gingerich, 1989: fig. 36B) the body of the mandible PAT 159 only slightly  
606 increases in height posteriorly between p3 and m3. The downward curve of the anterior part  
607 of the mandible, anterior to p2 at the level of p1 (that is of the symphysis) observed on PAT  
608 159 is neither present on the specimen of *D. pakistanensis* illustrated by Thewissen et al.

609 (1983: pl. 2.4a) nor on that of *D. indicus* illustrated by Kumar et al. (2010: fig. 5G). This  
610 downward slope of the anterior-most region of the mandible is however perceptible on the  
611 occluding tooth row of *D. pakistanensis* (Thewissen et al., 1983: pl. 1.3a) and is observed in  
612 other artiodactyls of the Eocene (e.g. *Chorlakkia* Gingerich et al., 1979). The main mental  
613 foramina observed on the labial surface of PAT 159 are also present in the other *Diacodexis*  
614 species. The space between the root of the ascending ramus and the posterior edge of m3 is  
615 superior in PAT 159 than in other *Diacodexis* species for which this character is documented  
616 (*D. pakistanensis*, Russell et al., 1983; *D. ilicis*, Kumar et al., 2010).

617 Comparison of the tooth row with other early-middle Ypresian *Diacodexis* species.

618 The dentition of *D. cf. gigasei* can only be partially compared to other European *Diacodexis*  
619 species because its upper dentition is not documented, and because lower premolars of most  
620 of the other *Diacodexis* species are not documented: the p3 can only be compared to *D.*  
621 *antunesi*, *D. gazini* and *D. aff. antunesi*, the p4 can only be compared to *D. morrissi*. In terms  
622 of size, the dental remains of *D. cf. gigasei* from Palette are generally larger than those of *D.*  
623 *antunesi*, and close in size to other MP7 species from Southern Europe (Fig. 4).

624 Comparison with Southern European MP7 and MP8+9 species. The lower dentition  
625 of *D. cf. gigasei* shows clear differences with that of *D. antunesi*. The p3 has a longer  
626 preprotocristid, more curved lingually than the p2/3? of *D. antunesi*, which is also labio-  
627 lingually slenderer. These differences can be due to the fact that SNC 64 is in fact a p2 rather  
628 than a p3. Concerning the lower molars, compared to *D. antunesi*, *D. cf. gigasei* presents a  
629 proportionally smaller trigonid that represents less than half of the crown surface. The  
630 trigonid basin is slender, and shallower and the paraconid is very close to the metaconid. The  
631 postectometacristid is absent in *D. cf. gigasei* whereas it is long sharp and connected to the  
632 ectoentocristid in *D. antunesi*. The cingulids of *D. cf. gigasei* are longer and the anterior  
633 cingulid is almost connected posteriorly to the labial one. The hypoconulid is located closer to

634 the median plane of the tooth in *D. cf. gigasei*. In this latter taxon, there is a marked  
635 difference of height between the protoconid and the lingual cuspids, whereas in *D. antunesi*  
636 this difference is weaker. The astragalus of *D. cf. gigasei* from Palette is more robust than that  
637 of *D. antunesi* (Fig. 2 vs Fig. 10, Table 2). The narrowing at the level of its neck is less  
638 pronounced and the tibial trochlea groove is wider and the sulcus tali narrower than in *D.*  
639 *antunesi*. Compared to *D. aff. antunesi* from Fordones, the p3 of *D. cf. gigasei* presents much  
640 smaller paraconid and hypoconulid, and a longer preprotocristid, more curved lingually. The  
641 lower m1-2 of *D. cf. gigasei* are wider with longer cingulids and a more medial position of  
642 the hypoconulid. Compared to *D. gazini*, the p3 of *D. cf. gigasei* shows a wider protoconid  
643 than that of the p2/3? of the former species, a more central/medial position of the paraconid  
644 which is fused to the anterior cingulid. The tooth is labio-lingually slenderer in *D. gazini*.  
645 These differences might be due to the fact that RI 208 is in fact a p2 rather than a p3. The m2  
646 of *D. cf. gigasei* differs from that of *D. gazini* by a wider and lower crown; *D. gazini* shows a  
647 proportionally slenderer and smaller trigonid relative to the talonid and a longer anterior  
648 cingulid. Like in *D. gazini*, *D. cf. gigasei* has a paraconid very close to the metaconid.  
649 Compared to *D. cf. gigasei*, *D. varleti* presents a hypoconulid of m1-2 situated closer to the  
650 entoconid, a protoconid almost as high as the metaconid on lower molars, a shorter anterior  
651 cingulid, sharper lingual crests (postectometacristid absent in *D. cf. gigasei*). The groove  
652 separating the metaconid and the paraconid is deeper in *D. varleti* than in *D. cf. gigasei*.  
653 Finally, *D. cf. gigasei* differs from *D. corsaensis* by a smaller size of the p4 and larger size of  
654 m3 (Fig. 4).

655 *Comparison with Northern European MP7 species.* The *Diacodexis* material from  
656 Palette is close to *D. gigasei* from Dormaal (Belgium) in its size, and morphologically  
657 speaking by the presence of: i) a long anterior cingulid on m2, ii) a reduced lingual cutting  
658 edge on lower molars (low ectoendocristid and no clear postectometacristid), iii) an

659 hypoconulid apart from entoconid on m1-2, iv) a postentocristid directed toward the  
660 hypoconulid on m3. Lower molars from the two localities differ by their length/width ratios  
661 which are smaller for m1-2 of *D. cf. gigasei* than in those from Dormaal (Fig. 4). In *D. cf.*  
662 *gigasei*, the m3 paraconid also appeared reduced and the molar crown looks slightly more  
663 bunodont, but this can be due to difference in wear stages. As a result, despite the good  
664 morphological and close metrical correspondence between the material from Palette and that  
665 collected from Dormaal, the *Diacodexis* material from the former locality is left under open  
666 nomenclature as *D. cf. gigasei*. Further discoveries, especially that its upper molars, could  
667 clarify this attribution.

668         The p4 of *D. cf. gigasei* differs from that of *D. morrisi* (Hooker, 2010: fig. 47d,g) by a  
669 longer preprotocristid, more curved lingually, and by a shorter postectoprotocristid. Both taxa  
670 present three posterior crests originating from the protoconid, endoprotocristid,  
671 postprotocristid and postectoprotocristid. The m1 of *D. morrisi* shows a more open trigonid  
672 basin with a larger paraconid located more lingually than in *D. cf. gigasei*. The labial notch, in  
673 occlusal view, is deeper on m1 and m3 in *D. morrisi* and a long and sharp postectometacristid  
674 is present.

675         *Comparison with Northern American and Asian species.* *D. cf. gigasei* is smaller than  
676 *D. indicus* and all Northern American species; moreover, it has no postectometacristid in  
677 contrast to all North American and Asian species; it differs from *D. parvus* and *D. indicus* by  
678 a more central location of the hypoconulid. Finally, *D. indicus* and *D. pakistanensis* have a  
679 more labial cristid obliqua. The p4 of *D. cf. gigasei* differs from that of *D. ilicis* and *D. secans*  
680 *primus* in lacking a distinct lingual demarcation/inflexion of the paraconid. In *D. ilicis*, the  
681 lingual basin on the talonid is deeper and bordered by a thick posterior cingulid. The presence  
682 of the three posterior crests on p4 cannot be ascertained based on the low resolution figures  
683 provided by Rose et al. (2012) and Krishtalka and Stucky, (1985). There seem to be a stronger

684 endoprotocristid and no postectoprotocristid on the North American specimens.

685

686 *3.4. New material from the locality of La Borie, Aude, France.*

687 *Diacodexis* sp.

688 Fig. 11

689 **Referred material** (coll. UM): BRI 1, P3 (right); BRI 2, P4 (left); BRI 3, M2 (right); BRI 4,  
690 M3 (right); MHNT.PAL.2017.21.2, m2 on a fragmentary dentary (left).

691 **Locality and horizon:** La Borie, Aude, France; «Argiles rutilantes d'Issel et de Saint-Papoul»  
692 Formation, early Eocene, ~MP8+9.

693 **Description:** The unique lower molar is much worn; considering the size of its trigonid and  
694 the morphology of the preserved roots of the anterior teeth, MHNT.PAL.2017.21.2 is  
695 attributed to an m2. No peculiar detail of the crown is visible.

696 The upper dentition is documented by premolars and molars. The P3 (BRI 1) has a  
697 triangular outline (Fig. 11(D)) and three distinct roots (anterior, posterior, lingual). The  
698 paracone bears sharp and high pre- and post- paracristae, crenulation cannot be observed  
699 because of wear. There is no trace of parastyle, but the corresponding locus is slightly worn; if  
700 present, it was very small. There is no metastyle. The lingual lobe is large and protrudes  
701 lingually; it bears a small protocone and a small basin. The lingual cingulum is continuous  
702 and joins the anterior and posterior cingula. The labial cingulum is very thin. The P4 (BRI 2)  
703 has no ectoflexus (Fig. 11(C)). This tooth is remarkably unworn. The unworn paracone is  
704 very high. Parastyle and metastyle are present, the metastyle being higher than the parastyle.  
705 The P4 has a small protocone which summit is slightly anterior to that of the paracone. It  
706 bears anterior and posterior cristae. There are no endoproto- and endopara- cristae, nor  
707 anterior and posterior cingula.

708 The M2 (BRI 3) is only little worn but is broken anterolingually (Fig. 11(B)). It has

709 round labial corners. The labial edge is straight. The paracone is higher and slightly larger  
710 than the metacone. The preparacrista and postmetacrista are both on the same plane as the  
711 centrocrista. The endoparacristule and endometacristule are present, but the endoparacristule  
712 is very low. There is not a postmetacristule deflection (i.e. postmetacristule protruding on the  
713 posterior edge of the tooth, cf. Fig. 7B, F) on the occlusal surface. The styles are limited to  
714 cingular swellings. The posterior cingulum is short, there is no clear hypocone. The M3 (BRI  
715 4) is little worn. It has round labial corners and a tilted lingual edge (Fig. 11(A)). The  
716 paracone is the highest cusp. The preparacrista and postmetacrista are both on the same plan  
717 as the centrocrista. The anterior and posterior cingula are long, thick, but not connected at the  
718 protocone level.

719 **Remarks:**

720 Comparison with Southern European MP7 and MP8+9 species. The taxon from La  
721 Borie is larger than *D. antunesi* and smaller than *D. morrisi*. It differs from *D. antunesi* and *D.*  
722 *gigasei* in having no postmetacristule deflection on the occlusal surface. It differs from *D.*  
723 *antunesi* in having a P3 with an elongate paracone and more convex labial edge, a reduced  
724 parastyle on upper molars. It differs from other species of *Diacodexis* in having a P4 without  
725 anterior and posterior cingula. It differs from *D. gigasei* in having a P4 without ectoflexus and  
726 upper molars with shorter posterior cingulum (no lingual bulge). It differs from *D. morrisi* in  
727 having no endoparacrista and a less important groove intersecting the postprotocrista on upper  
728 molars.

729 The material of La Borie appears close to *D. gazini* in size and morphology. Both  
730 species have round labial corners on upper molars, straight labial edge on M2, and similar  
731 mesiodistal M2 length. On M3 however, the *Diacodexis* species from La Borie has a less  
732 protruding parastyle and strongly round cusps and conules when compared to *D. gazini*.  
733 Conversely, the M2 of La Borie does not show bulbous cusps like for the M3 of *D. gazini*.

734 This discrepancy could be explained by the degree of wear (the M2 is almost unworn contrary  
735 to the M3). Finally, the M2 from La Borie does not have a long and thick posterocingulum  
736 shaping in hypocone while the presence of the latter feature constitutes a diagnostic character  
737 of *D. gazini*. Finally, compared to *D. varleti*, the species from La Borie has less pronounced  
738 ectoflexus on M2, the parastyle is not protruding, and the conules are reduced with lesser  
739 endocristules.

740 Comparison with Northern American and Asian species. The taxon from La Borie is  
741 smaller than *D. indicus* and all North American species; it further differs from *D. ilicis* in  
742 having no postmetacristule deflection. Among Asian species, *Diacodexis* sp. from Andarak 2  
743 and *D. pakistanensis* differ from *Diacodexis* sp. from La Borie by the lack of endoparacristule  
744 and postprotocrista on upper molars and P4, respectively; *Diacodexis indicus* has a larger  
745 parastyle on M2 and a more reduced metacone on M3.

746

## 747 **4. Discussion**

### 748 *4.1. Ancestral morphotype of artiodactyl enamel microstructure*

749 Recent data on artiodactyl enamel microstructures revealed a diversity of patterns  
750 relevant to phylogenetic inferences (Alloing-Séguier et al., 2014). From this point of view,  
751 *Diacodexis* is crucial to discuss the enamel ancestral morphotype of artiodactyls. Since Maas  
752 and Thewissen (1995) and Stefen (1999), *Diacodexis* is thought to have developed a two-  
753 layered Schmelzmuster (the spatial arrangement of the different enamel types through enamel  
754 thickness): a thin layer (5-10%) of radial enamel close to EDJ and a thick layer of Hunter-  
755 Schreger bands (HSB) that generally extends to the EOS; in some parts a very thin layer of  
756 radial enamel can occur at the EOS. Our data on *Diacodexis antunesi* and *Diacodexis aff.*  
757 *antunesi*, which have a one-layered Schmelzmuster with ‘basic’ radial enamel only, reveal a



758 simple enamel pattern. This result implies a surprising interspecific variability among  
759 *Diacodexis* species, which is rare among eutherian mammals.

760 Maas and Thewissen (1995) based their observations on *Diacodexis* on an  
761 undetermined North American species represented by a lower molar from the Wa-5 (=   
762 ‘*Bunophorus* Interval Zone’ in the original publication). Regarding Stefen (1999)’s analysis,  
763 two species were studied based on specimens from the UCMP collections, i.e. *Diacodexis*  
764 *robustus* and an undetermined species. Theodor et al. (2007) now attribute the former species  
765 to *Bunophorus*; this diacodexeid genus is thus excluded from the present discussion. As for  
766 the undetermined *Diacodexis*, online UCMP database (accessed on September 2017, available  
767 at: <http://ucmpdb.berkeley.edu/>) indicates that the figured specimen comes from the mid-  
768 Wasatchian (Wa3-5) (= ‘Graybullian’ in the database) of the Willwood Formation, Wyoming.  
769 Therefore, based on the stratigraphical ranges proposed by Krishtalka and Stucky (1985) for  
770 North American *Diacodexis* species, we can assume that the undetermined species studied by  
771 Maas and Thewissen (1995) and Stefen (1999) is either *D. secans* (known from the early  
772 Wasatchian to the Bridgerian) or less probably *D. gracilis* (rare, known in the mid-  
773 Wasatchian, Wa3-5). Importantly, *Diacodexis antunesi* and *Diacodexis* aff. *antunesi* are  
774 smaller and have more crestiform, simple molars than *D. secans* and *D. gracilis*. These size  
775 and morphological differences could be correlated to the dissimilar enamel microstructure that  
776 we observe between *Diacodexis* species.

777 Actually, according to Koenigswald et al. (1987), HSB characterized almost all large  
778 herbivorous mammals since the early Paleocene. Stefen (1999) proposed that convergent  
779 evolution of HSB within eutherians result of co-occurring changes in dental morphology,  
780 body-size, overall ecology, and chewing pattern. Fundamentally, small insectivorous  
781 mammals have ‘basic’ radial enamel (e.g., eulipotyphlans, chiropterans, small primates, some  
782 “condylarths”) whereas herbivorous, omnivorous, and mid-sized carnivorous and large

783 mammals have prism decussation such as HSB. Interestingly, our results on *Diacodexis*,  
784 would support this trend at the genus level: *D. antunesi* and *D. aff. antunesi* are small-sized  
785 most likely insectivorous species with tribosphenic, crestiform molars, whereas *D. secans* and  
786 *D. gracilis* are putative omnivorous and/or herbivorous, larger species with more  
787 quadritubercular, bunodont molars (see also Theodor et al. 2007: p. 37).

788 Interestingly also, the fossil record of placental mammals suggests that the ‘basic’  
789 radial enamel is the primitive condition (see Tabuce et al. 2017: p. 103). With the exception  
790 of odontocetes (due to the simplification of their tooth morphology and piscivorous diet),  
791 there are no reversion from HSB to ‘basic’ radial enamel. In other words, the enamel  
792 microstructure (i.e., ‘basic’ radial enamel) of *Diacodexis antunesi* most likely represents the  
793 primitive condition among *Diacodexis* species and most probably represents the ancestral  
794 morphotype for Artiodactyla.

795

#### 796 4.2. Ancestral morphotype of artiodactyl fourth lower deciduous premolar

797 The new *Diacodexis* material described here includes one dp4 attributed to *D. aff*  
798 *antunesi* (Figs. 8A-C, 12A). This specimen from the Ypresian locality of Fordones represents  
799 one of the earliest record of dp4 for artiodactyls. Only few specimens of dp4 of *Diacodexis*  
800 are documented in the literature. A dp4 of *D. varleti* was reported by Sudre et al. (1983) from  
801 Condé-en-Brie, but the specimen was neither figured nor described by the authors, and could  
802 not be found in the MNHN collections. In addition to this specimen, a dp4 of *D. morrissi* has  
803 been described and figured by Hooker (2010: fig. 48E). This specimen is fresh and allows  
804 observing the finest structures of the crown (Fig. 12(B)). In addition to these specimens,  
805 several dp4s of early artiodactyls are documented from the French MP10 locality of  
806 Prémontré (Aisne, Northern France). One specimen, SLP-29-PE 637 (Fig. 12(E)), was  
807 originally attributed to *D. cf. varleti* by Sudre and Erfürt (1996) but it was not figured. Four

808 other dp4 of artiodactyls from the same locality were referred to Dichobunidae Eurodexeinae  
809 by Sudre and Erfürt (1996: pl. 1, fig. 8; Fig. 12(F)). Since the publication of this material,  
810 another specimen was retrieved from the sediment from Prémontré. This specimen, UM  
811 PRE151, is here attributed to *Diacodexis* sp. (Fig. 12(D)). From Asia, a worn dp4 of *D.*  
812 *indicus* was described by Kumar et al. (2010: fig. 6G-I; Fig. 12(C)) from the Vastan mine in  
813 Western India. Lockett and Hong (1998) paid special attention to the morphology of the lower  
814 fourth deciduous premolar in extant and fossil artiodactyls. In artiodactyls, the anterior lobe of  
815 the trilobed dp4 is described as bearing a mesiolabial and a mesiolingual cusp, forming a third  
816 lobe, a character retrieved as a synapomorphy of Artiodactyla (e.g., Gentry and Hooker, 1988;  
817 Lockett and Hong, 1998). Lockett and Hong (1998) consider that the paraconid is anteriorly  
818 displaced and lingual, and that “*the anterior lobe of the artiodactyl dP<sub>4</sub> is characterized by the*  
819 *development of a neomorphic cusp on the paracristid that runs between the protoconid and*  
820 *the paraconid; this new cusp provides a "squaring" of the anterior portion of the tooth*”  
821 (Lockett and Hong, 1998: p. 135). Surprisingly, these authors illustrate a specimen they refer  
822 to as *Diacodexis* cf. *varleti* from the French locality of Prémontré and numbered SLP 29PR  
823 2122, while this specimen was initially attributed to Eurodexeinae indet. by Sudre and Erfürt  
824 (1996). A line drawing of the occlusal surface of the crown of SLP 29PR 2122 (Fig. 12(F))  
825 shows that its general pattern considerably differs from that of dp4 of other *Diacodexis*  
826 species and that this specimen might indeed belong to the Eurodexeinae. In turn, as illustrated  
827 on Figure 12, the MP7 European specimens referred to *Diacodexis* all present only one large  
828 cusp on what is generally considered as the anterior lobe or “paraconid lobe” (Hooker,  
829 2010). This cusp is located on the lingual border of the tooth, and bears its own crest pattern  
830 with a lingual and a labial crest, touching the premetacristid and the preprotocristid  
831 respectively. According to its lingual position, this anterior cusp might be called the  
832 paraconid. The anterior part of the tooth rather has a triangular shape and there is no

833 "squaring" of the anterior portion of the tooth, as described by Hooker (2010: p. 108) based  
834 on the specimen of *D. morrisoni*. The general shape of the crown is hourglass rather than  
835 trilobed, and there is no constriction between the paraconid lobe and the rest of the trigonid.  
836 In the specimens of *Eurodextis russelli* from Prémontré (Sudre and Erfürt, 1996: pl. 1, fig. 8),  
837 an additional cuspid is present labial to the large paraconid and the anterior part of the tooth is  
838 indeed squared; it presents a trilobed outline, like in most other extant and extinct artiodactyls.  
839 On the very fresh dp4 of *Diacodextis* sp. from Prémontré (UM PRE151, Fig. 12(D)), a very  
840 small accessory cuspid is present on the labial crest originating from the paraconid. The dp4  
841 from the same locality attributed to *Diacodextis* cf. *varleti*, by Sudre and Erfürt (1996) in fact  
842 presents a completely different morphology: there is one main cusp which is displaced  
843 labially and connected to the protoconid, a series of accessory cuspids are present in a crest-  
844 like structure, not mesiolabially, but lingually (Fig. 12(E)). There is no anterior basin. These  
845 two specimens illustrate the potential intraspecific variation for dp4.

846         These observations suggest that the labial anterior cuspid appears after the lingual one,  
847 here recognized as the paraconid based on its lingual position. Then it seems logical to  
848 recognize the anterior lingual cuspid as the paraconid and the labial one as the primonid, as  
849 identified by Luckett and Hong (1998). This nomenclature however contrasts with that used  
850 by authors for other artiodactyl groups such as suoids (Made, 1996; Orliac and Ducrocq,  
851 2012; Orliac et al., 2015) where the labial cusp is named the paraconid and the lingual one the  
852 primonid. Early European *Diacodextis* dp4s suggest the opposite homology. In the  
853 phylogenetic analyses of Theodor and Foss (2005), the dp4 of *Diacodextis* is considered to be  
854 six cusped based on observations of *Diacodextis pakistanensis*. In contrast, observations of  
855 Ypresian material from Europe indicate that early *Diacodextis* species have only one anterior  
856 cuspid on dp4. Besides, the presence of two basins only, and the hourglass outlines of the dp4  
857 of earliest *Diacodextis* species, do not match the trilobed pattern traditionally considered as a

858 synapomorphy for Artiodactyla. Finally, the dp4s of *Diacodexis* bear two pillars only, which  
859 contrasts with the three rooted pattern of most more derived artiodactyls. The presence of a  
860 two rooted pattern also occurs in other early members of Artiodactyla (Dichobunidae,  
861 Cainotheriidae, Choeropotamidae; Orliac pers. obs.) as well as in basal members of Suoidea  
862 (Orliac et al., 2012), and might represent the primitive condition within Artiodactyla.

863

#### 864 4.3. Relationships within *Diacodexis* and paleobiogeographic inferences

865 Artiodactyls appear rather abruptly in earliest Eocene deposits in the fossil record  
866 (Gingerich, 2006). Because of their early occurrence and the simple tribosphenic pattern of  
867 their molars, *Diacodexis* has been regarded as a paraphyletic ancestral pool of species near the  
868 base of the artiodactyl radiation (Rose, 2006), and was considered as implicated in the origin  
869 of some European Eocene endemic groups (Sudre and Erfurt, 1996; Checa Soler, 2004), as  
870 well as North American groups (Krishtalka and Stucky, 1985). The position of *Diacodexis*  
871 species varies depending of the sample included in phylogenetic analyses (e.g., Theodor and  
872 Foss, 2005; Geisler et al., 2007; Orliac and Ducrocq, 2012).

873 *Diacodexis* shows a vast repartition of species, close in terms of morphology and  
874 stratigraphic age, despite sometimes huge geographic distances. For several taxa, mostly for  
875 European ones, only few specimens are available. On the other hand, species documented by  
876 relatively abundant material indicate that intraspecific variation occurs and might affect  
877 features used to differentiate species (e.g., morphology of the m3 talonid, of the cingulids).  
878 Besides, the absence of complete skull, or even tooth raw preservation, makes association of  
879 upper and lower dentition problematic for some taxa (e.g., *Diacodexis* cf. *varleti*; Sudre et al.,  
880 1983: p. 302). In addition to these taphonomic/preservation bias, wear degree has a potentially  
881 drastic impact on crown morphology and the way it can be described by authors. Several  
882 features, such as relative height or size of cusp(id)s, or accessory crest pattern can be affected

883 by wear. To be reliable, comparisons should be performed between specimens showing the  
884 same degree of wear, which is not always possible given the scarcity of available material for  
885 some taxa.

886         The new material described here shows that premolars, deciduous dentition, as well as  
887 enamel microstructure are informative for systematic and phylogenetic purposes. However,  
888 these characters are incompletely represented in several *Diacodexis* species, limiting the  
889 extent of comparisons. Their rather simple molar morphology, combined to potential  
890 intraspecific variation, dental locus association problems, impact of wear on morphology,  
891 continuity of most of the characters described (cusp/id bulging, relative size, height, conule  
892 location, cingulum/id size, length), and to the incompleteness of the loci documented between  
893 localities/taxa, are factors that hinder the implementation of a phylogenetic analysis of  
894 *Diacodexis* species so far.

895         Yet, relationships of European *Diacodexis* species have been discussed in the literature  
896 based on comparisons between taxa only and not on formal cladistic analyses. *D. antunesi* has  
897 been regarded as the most primitive *Diacodexis* species by some authors (e.g. Smith et al.  
898 1996; Theodor et al., 2007); Hooker (2010) instead considers that *D. gigasei* from Dormaal  
899 (MP 7) represents the most primitive species of the genus. Based on outgroup comparison  
900 polarization criterion with hyopsodontid and arctocyonid ‘condylarths’, Hooker (2010)  
901 considers that some characters point to *D. antunesi* being relatively derived within *Diacodexis*  
902 species. These characters are: on lower molars, the crown height, the lingual position of the  
903 m1-2 hypoconulid, the constriction of the m3 hypoconulid lobe, and the bulging of m1-2  
904 entoconid; and on upper molars, the occlusal pattern of distolabially directed M1-2  
905 postprotocrista, and a “bowed centrocrista”. The lower molars of *D. antunesi* indeed present a  
906 hypoconulid closer to the entoconid and located more lingually than what is observed in *D.*  
907 *gigasei*. For this character *D. antunesi* is closer to *D. varleti* from Condé-en-Brie, France, but

908 also to *D. indicus* from Vastan, India (Fig. 13). However, based on our observations, the  
909 entoconid of *D. antunesi* does not appear to be particularly larger than that of *D. gigasei* on  
910 m1 (Fig. 13(B) vs (F)). Smith et al. (1996) propose that *D. gigasei* and *D. antunesi* share a  
911 continuous structure uniting the hypoconulid and the hypoconid, a character seen by these  
912 authors as plesiomorphic. This continuous structure might result from wear pattern on the  
913 specimens, yet, study of fresh teeth indicates that the hypoconulid and the hypoconid are  
914 always separated by a groove (Fig. 13). For upper molars, the “bowing of the centrocrista”  
915 mentioned by Hooker (2010), is, to us, directly related to the size of the parastyle, which is  
916 large in *D. antunesi*; while the orientation of the preprotocrista relies more on the general  
917 lingual width of the upper molars (i.e. wide in *D. ilicis* and *D. gigasei*). Again, for these  
918 characters, *D. antunesi* is closer to Asian taxa, *D. indicus* and *D. pakistanensis* (Kumar et al.,  
919 2010: fig. 8), which present a lingual shift of the preprotocrista on M1, and a relatively  
920 narrow lingual lobe on the upper molars. Based on upper molar morphology, we agree that *D.*  
921 *gigasei* and *D. morrissi* are closer to *D. ilicis* than to *D. antunesi*. Yet, for now, there is no  
922 formal way to affirm that these character state represent the primitive condition.

923         Hooker (2010) uses outgroup comparison as polarization criterion, and compares  
924 *Diacodexis* species to hyopsodontids and arctocyonids. Hyopsodontids is a polyphyletic  
925 assemblage and might be more closely related to Perissodactyla or some afrotherians, than to  
926 Artiodactyla (Zack et al., 2005; Tabuce et al., 2007b; Ladevèze et al., 2010; Tabuce in press)  
927 and should be left aside. Arctocyonids show a wide range of morphologies, including a  
928 hypoconid closely apposed to the entoconid in lingual position on m1-2, and bulging  
929 entoconid (e.g., *Chriacus truncatus* Rose, 1996: fig. 1; *Loxolophus hyattianus* Kondrashov  
930 and Lucas, 2012). Arctocyonids also show a wide range of orientation of the M1-2  
931 postprotocrista and “centrocrista bowing”: *Protungulatum* and other arctocyonids (e.g., Rose,  
932 2006: fig. 12.3) exhibit a lingual shift of the preparacrista and a strong parastyle, related to a

933 “bowed centrocrista”. This is a plesiomorphic condition at the eutherian scale (e.g., Wible et  
934 al., 2009). The generally simple molar crown morphology of most arctocyonids, with high  
935 and pointed cusps associated with the primitive tribosphenic-tritubercular pattern, recall a  
936 somewhat more “insectivorous” diet. Still, this morphology could as well be secondarily  
937 derived within Artiodactyla, but in the general picture of Paleocene/Eocene eutherians, would  
938 be consistent with a primitive pattern in *D. antunesi*.

939         The new material described here further documents the premolar dentition of  
940 European *Diacodexis* species and provides new morphological characters for comparisons.  
941 The P4 of *D. antunesi*, is morphologically close to *D. pakistanensis* with a labial wall with no  
942 ectoflexus, and a paracone with salient endoparacristule. This structure is absent in *D. gigasei*,  
943 and in the specimen referred to *D. aff. antunesi* from Fordones; it is also lacking in *D. ilicis*.  
944 The P4 of *D. gigasei* presents an ectoflexus, like North American species like *D. ilicis* (Fig.  
945 7), *D. secans-metsiacus* (Krishtalka and Stucky, 1985: fig. 4D-E).), or *D. secans-secans*  
946 (Krishtalka and Stucky, 1985: fig. 2A-B). The P3 of European species is rather short  
947 anteroposteriorly and bears a wide paracone; the lingual lobe of *D. aff antunesi* is small and  
948 poorly differentiated, and bears no accessory cusp. This lobe is larger and more individualized  
949 in *Diacodexis* sp. from La Borie, with a small accessory cusp. P3 of European species are  
950 closer morphologically to the P3 of *D. indicus* from Vastan, than to the P3 of North American  
951 species *D. ilicis* and *D. secans metsiacus*, which are longer anteroposteriorly and slenderer  
952 bucco-lingually with a more salient lingual lobe and a bigger accessory cusp. Regarding the  
953 lower dentition, the p4 of *D. aff. gigasei* from Palette is closer to *D. ilicis* than to *D. indicus*.  
954 Unfortunately, comparisons with *D. antunesi* are not possible as this locus is not documented  
955 yet. The morphology of the dp4 is complex and each documented taxon has its specificity (see  
956 above).



957 Our observations highlight that *D. gigasei* is morphologically closer to *D. ilicis* than to  
958 *D. antunesi*, in accordance with Gingerich (1989), Smith et al. (1996), and Hooker (2010).  
959 *Diacodexis antunesi*, and *D. aff. antunesi* from Fordones appear to be morphologically closer  
960 to the Asiatic taxa *D. indicus* and *D. pakistanensis*. As a result, if a cladistic analysis of these  
961 taxa appears premature, an interesting conclusion may nevertheless be drawn at this stage:  
962 although *D. antunesi* and *D. gigasei* are certainly very close in age, close to the PETM, the  
963 preceding comparisons show that these two European species differ widely. This strongly  
964 suggests that at least two phases of migration of *Diacodexis* could have occurred in Europe  
965 around the Paleocene-Eocene boundary. Asia might be the dispersal centre of these two  
966 events (see Beard 1998). Interestingly, an Asian origin of European *Diacodexis* might be  
967 supported by the similarities between *D. antunesi* and the Asian species *D. pakistanensis* and  
968 *D. indicus*. Such a faunal interchange between Europe and South Asia, but well after the  
969 Paleocene-Eocene boundary, is also well-supported by some recent evidence (e.g., Smith et  
970 al. 2007; Rana et al. 2008; Rose et al. 2009; Tabuce et al. 2009).

971 Finally, we found numerous similarities between *D. cf. gigasei* from Palette and *D.*  
972 *gigasei* from Dormaal. This result is quite surprising considering the now well-established  
973 intra-European provincialism that characterizes the earliest Ypresian: mammals from the  
974 northwestern (Anglo-Belgian and Paris basins) and southwestern (south of France and Iberian  
975 Peninsula) provinces greatly differ (Marandat, 1997; Marandat et al., 2012; Solé et al., 2017).  
976 Along with few species —such as the herpetotheriid marsupial *Peratherium constans* and the  
977 paromomyid plesiadapiform *Arcius fuscus* (see Godinot et al. 1987; López-Torres and Silcox  
978 in press)— *D. gigasei* could be one of the rare species in common between northwestern and  
979 southwestern bioprovinces.

980

## 981 **5. Conclusions**

982           The new material described here considerably increases our knowledge of European  
983 *Diacodexis* species, including the earliest representatives of the genus. Documentation of the  
984 enamel microstructure of *Diacodexis antunesi* from Silveirinha and *Diacodexis* aff. *antunesi*  
985 from Fordones, reveals that those early species had a simple enamel pattern with one-layered  
986 Schmelzmuster composed of ‘basic’ radial enamel only. These observations contrast with  
987 those performed on North American species that present a two-layered Schmelzmuster  
988 composed of a thin layer of radial enamel and a thick layer of Hunter-Schreger bands. This  
989 latter enamel microstructure pattern was so far considered to represent the primitive condition  
990 within Artiodactyla. The occurrence of a simple one-layer enamel in earliest European  
991 *Diacodexis* species challenges this hypothesis, and rather suggests that this simple pattern  
992 represents the primitive condition among *Diacodexis* species and probably among  
993 Artiodactyla. Likewise, the crown morphology of the dp4 of earliest *Diacodexis* species  
994 indicates a considerable diversity of the tooth occlusal pattern. Some *Diacodexis* species from  
995 Europe have only one anterior cuspid, two basins, and present an hourglass outline instead of  
996 the trilobed pattern so far considered as a synapomorphy for Artiodactyla. Besides, the dp4 of  
997 *Diacodexis* bear two pillars only, which contrasts with the three rooted pattern of other  
998 artiodactyls considered to be more derived. Study of earliest *Diacodexis* species therefore  
999 questions features considered as primitive within Artiodactyla. A large scale revision of  
1000 diacodexeid species including North American material, as well as a wide sampling of  
1001 potential branching groups, would be necessary to discuss the early radiation of Artiodactyla  
1002 through a formal cladistic analysis, and properly determine character polarization.

1003           In accordance with previous study, our observations highlight that *Diacodexis gigasei*  
1004 is morphologically closer to *D. ilicis* than to *D. antunesi*. The latter species, together with the  
1005 new material referred to *D. aff. antunesi* from Fordones, appear to be morphologically closer  
1006 to the Asiatic taxa *D. indicus* and *D. pakistanensis*. Finally, we found numerous similarities

1007 between *D. cf. gigasei* from Palette and *D. gigasei* from Dormaal, a result that attenuates the  
1008 intra-European provincialism that characterizes the earliest Ypresian. *Diacodexis gigasei*  
1009 could be one of the rare species in common between northwestern and southwestern  
1010 bioprovinces.

1011

## 1012 **Acknowledgements**

1013 We are grateful to A.-L. Charuault (ISEM, Montpellier, France) for having prepared  
1014 the mandible from Palette and to J. Clavel (IBENS, Paris, France) for providing us with  
1015 photographs from the Silveirinha material. We are also grateful to the Rougier family, who  
1016 facilitated field work in Palette. We thank L. Alloing-Séguier (ISEM) and S. Enault (ISEM)  
1017 for their advices regarding enamel microstructure protocol and taking images. Data presented  
1018 in this work were produced through the technical facilities of the MRI platform and of the  
1019 labEx CeMEB. We warmly thank Chantal Cazevieille (Montpellier RIO Imaging, Institut des  
1020 Neurosciences de Montpellier, France) for granting access to a scanning electron microscope  
1021 facility. We are grateful to the Terreal Society, especially L. Nathan for his assistance during  
1022 the excavations.

1023

## 1024 **References**

- 1025 Alloing-Séguier, L., Lihoreau, F., Boisserie, J. R., Charruault, A. L., Orliac, M., Tabuce, R.,  
1026 2014. Enamel microstructure evolution in anthracotheres (Mammalia, Cetartiodactyla)  
1027 and new insights on hippopotamoid phylogeny. *Zoological Journal of the Linnean*  
1028 *Society*, *171*(3), 668-695.
- 1029 Antunes, M.T., Russell, D.E., 1981. Le gisement de Silveirinha (Bas mondego, portugal) : la  
1030 plus ancienne faune de Vertébrés éocènes connue d'Europe. *Comptes Rendus de*  
1031 *l'Académie des Sciences II* 293, 1099–1102.
- 1032 Antunes, M.T., Casanovas, M.L., Cuesta, M.A., Checa, L., Santafé, J.V., Agustí, J., 1997.  
1033 Eocene mammals from Iberian Peninsula. *Mémoires et travaux de l'Institut de*  
1034 *Montpellier*, 21, 337–352.

- 1035 Averianov, A., 1996. Artiodactyla from the early Eocene of Kyrgyzstan. *Palaeovertebrata*,  
1036 25(2-4), 359–369.
- 1037 Bajpai, S., Kapur, V.V., Das, D.P., Tiwari, B.N., Saravanan, N., Sharma, R., 2005. Early  
1038 Eocene land mammals from the Vastan lignite mine, district Surat (Gujarat), Western  
1039 India. *Journal of The Palaeontological Society of India* 50 (1), 101–113.
- 1040 Beard, K.C., 1998. East of eden: Asia as an important center of taxonomic origination in  
1041 mammalian evolution. *Bulletin of Carnegie Museum of Natural History* 34, 5–39.
- 1042 Biochrom'97. 1997. Synthèses et tableaux de corrélations, in : Aguilar, J.P., Legendre, S.,  
1043 Michaux, J. (Eds.), Actes du congrès international de biochronologie mammalienne  
1044 Biochrom' 97. Mémoires et travaux de l'institut de Montpellier, Ecole Pratique des  
1045 Hautes Etudes 21. Montpellier, 1997, pp. 765–805.
- 1046 Boisserie, J.-R., Lihoreau, F., Orliac, M.J., Fisher, R., Weston, E., Ducrocq, S., 2009.  
1047 Morphology and phylogenetic relationships of the earliest known hippopotamids  
1048 (Cetartiodactyla, Hippopotamidae, Kenyapotaminae). *Zoological Journal of the Linnean*  
1049 *Society*, 158, 325–367.
- 1050 Bowen, G.J., Maibauer, B.J., Kraus, M.J., Röhl, U., Westerhold, T., Steimke, A., Gingerich,  
1051 P.D., Wing, S.L., Clyde, W.C., 2015. Two massive, rapid releases of carbon during the  
1052 onset of the Palaeocene–Eocene thermal maximum. *Nature Geoscience*, 8, 44–47.
- 1053 Checa Soler, L.C., 2004. Revisión del género *Diacodexis* (Artiodactyla, Mammalia) en el  
1054 Eoceno inferior del Noreste de España. *Geobios*, 37(3), 325–335.
- 1055 Cope, E.D., 1882. The oldest artiodactyl. *American Naturalist*, 16, 61.
- 1056 Estravis, C., Russell, D.E., 1989. Découverte d'un nouveau *Diacodexis* dans l'Eocène  
1057 inférieur de Silveirinha, Portugal. *Palaeovertebrata*, 19 (1), 29–44.
- 1058 Estravis, C., 1992. Estudo dos mamíferos do Eocénico inferior de Silveirinha (Baixo  
1059 Mondego). Universidade Nova de Lisboa, Lisbon, p. 248.
- 1060 Estravis, C., 2000. Nuevos mamíferos del Eoceno inferior de Silveirinha (Baixo Mondego,  
1061 Portugal). *Coloquios de Paleontologia* 51, 281–311.
- 1062 Gatesy, J., Geisler, J. H., Chang, J., Buell, C., Berta, A., Meredith, R. W., et al., 2013. A  
1063 phylogenetic blueprint for a modern whale. *Molecular phylogenetics and evolution*,  
1064 66(2), 479–506.
- 1065 Geisler, J.H., Chang, J., Buell, C., Berta, A., Meredith, R.W., Springer, M.S., McGowen,  
1066 M.R., 2013. A phylogenetic blueprint for a modern whale. *Molecular phylogenetics and*  
1067 *evolution* 66, 479–506.

1068 Geisler, J.H., 2001. New morphological evidence for the phylogeny of Artiodactyla, Cetacea,  
1069 and Mesonychidae. *American Museum Novitates*, 1–53.

1070 Geisler J.H., Theodor, J.M., 2009. *Hippopotamus* and whale phylogeny. *Nature*, 468 (7236),  
1071 e1–e4.

1072 Gentry, A.W., Hooker, J.J., 1988. The phylogeny of the Artiodactyla, in: Benton, M.J. (Ed.),  
1073 The phylogeny and classification of the tetrapods, Volume 2: Mammals. Systematics  
1074 Association, Clarendon press, Oxford, pp. 235–272.

1075 Gingerich, P.D., 1989. New earliest Wasatchian mammalian fauna from the Eocene of the  
1076 Northwestern Wyoming: composition and diversity in a rarely sampled high-floodplain  
1077 assemblage. *University of Michigan, Papers on Paleontology*, 28, 1–97.

1078 Gingerich, P.D., Russell, D.E., Sigogneau-Russell, D., Hartenberger, J.L., 1979. *Chorlakkia*  
1079 *hassani*, a new middle Eocene dichobunid (Mammalia, Artiodactyla) from the Kuldana  
1080 Formation of Kohat (Pakistan). *Contributions from the Museum of Paleontology, The*  
1081 *University of Michigan*, 25(6), 117–124.

1082 Gingerich, P.D., 2006. Environment and evolution through the Paleocene–Eocene thermal  
1083 maximum. *Trends in Ecology and Evolution*, 21, 246–253.

1084 Gingerich, P.D., 1989. New earliest Wasatchian mammalian fauna from the Eocene of  
1085 northwestern Wyoming: composition and diversity in a rarely sampled high-floodplain  
1086 assemblage. *Papers on paleontology*, 28, 1–97.

1087 Godinot, M., 1981. Les mammifères de Rians (Eocène inférieur, Provence). *Palaeovertebrata*,  
1088 10(2), 43–126.

1089 Godinot, M., 1984. Un nouveau genre de Paromomyidae (Primates) de l'Eocène inférieur  
1090 d'Europe. *Folia Primatologica* 43, 84–96.

1091 Godinot, M., Crochet, J.-Y., Hartenberger, J.-L., Lange-Badré, B., Russell, D.E., Sigé, B.,  
1092 1987. Nouvelles données sur les mammifères de Palette (Eocène inférieur, Provence),  
1093 in: Schmidt-Kittler, N. (Ed.), *International Symposium on Mammalian Biostratigraphy*  
1094 *and Paleoecology of the European Paleogene*. Verlag Friedrich Pfeil, pp. 273–288.

1095 Guthrie, D.A., 1971. The mammalian fauna of the Lost Cabin Member, Wind River  
1096 Formation (Lower Eocene) of Wyoming. *Annals of Carnegie Museum*, 43(4), 47–90.

1097 Hooker, J.J., 2010. The mammal fauna of the early Eocene Blackheath Formation of Abbey  
1098 Wood, London. *Palaeontographical Society Monographs* 634 (164), 1–162.

1099 Koenigswald, W.V., Rensberger, J.M., Pfretzschner, U., 1987. Changes in the tooth enamel of  
1100 early Paleocene mammals allowing increased diet diversity. *Nature*, 328, 150–152.

- 1101 Kondrashov, P.E., Lucas, S.G., 2012. Nearly Complete Skeleton of *Tetraclaenodon*  
1102 (Mammalia, Phenacodontidae) from the Early Paleocene of New Mexico: Morpho-  
1103 Functional Analysis. *Journal of Paleontology*, 86 (1), 25–43.
- 1104 Krishtalka, L., Stucky, R.K., 1985. Revision of the Wind river Faunas, early Eocene of central  
1105 Wyoming, revision of *Diacodexis* (mammalia, artiodactyla). *Ann.als of the Carnegie*  
1106 *Museum* 54, 413–486.
- 1107 Kumar, K., Jolly, A., 1986. Earliest artiodactyl (*Diacodexis*, Dichobunidae: Mammalia) from  
1108 the Eocene of Kalakot, northwestern Himalaya, India. *Indian Society of Geology*  
1109 *Bulletin*, 2, 20–30.
- 1110 Kumar, K., Rose, K.D., Rana, R.S., Singh, L., Smith, T., Sahni, A., 2010. Early Eocene  
1111 artiodactyls (Mammalia) from western India. *Journal of Vertebrate Paleontology*, 30(4),  
1112 1245–1274.
- 1113 Ladevèze, S., Missiaen, P., Smith, T., 2010. First skull of *Orthaspidotherium edwardsi*  
1114 (Mammalia, “Condylarthra”) from the late Paleocene of Berru (France) and  
1115 phylogenetic affinities of the enigmatic European family Pleuraspidotheriidae. *Journal*  
1116 *of Vertebrate Paleontology*, 30(5), 1559–1578.
- 1117 Laurent, Y., Adnet, S., Bourdon, E., Corbalan, D., Danilo, L., Duffaud, S., Fleury, G., Garcia,  
1118 G., Godinot, M., Le Roux, G., Maisonnave, C., Métais, E., Mourer-Chauviré, C.,  
1119 Presseq, B., Sigé, B., Solé, F., 2010. La Borie (Saint-Papoul, Aude) : un gisement  
1120 exceptionnel dans l’Éocène basal du Sud de la France. *Bulletin de la Société d'Histoire*  
1121 *Naturelle de Toulouse* 146, 89–103.
- 1122 Luckett, W.P., Hong, N., 1998. Phylogenetic relationships between the orders Artiodactyla  
1123 and Cetacea: a combined assessment of morphological and molecular evidence. *Journal*  
1124 *of Mammalian Evolution*, 5(2), 127–182.
- 1125 López-Torres, S., Silcox, M., in press. The European Paromomyidae (Primates, Mammalia):  
1126 taxonomy, phylogeny, and biogeographic implications. *Journal of Paleontology*.
- 1127 Maas, M.C., Thewissen, J.G.M., 1995. Enamel microstructure of *Pakicetus* (Mammalia:  
1128 Archaeoceti). *Journal of Paleontology*, 69, 1154–1163.
- 1129 Made, J. van der., 1996. Listriodontinae (Suidae, Mammalia), their evolution, systematics and  
1130 distribution in time and space. *Mededelingen van de Werkgroep voor Tertiaire en*  
1131 *Kwartaire Geologie*, 33(1/4), 3–254.
- 1132 Marandat, B., 1991. Mammifères de l’Ilerdien moyen (Eocène inférieur) des Corbières et du  
1133 Minervois (Bas-Languedoc, France). *Systématique, Biostratigraphie, corrélations.*  
1134 *Palaeovertebrata*, 20(2-3), 55–144.

- 1135 Marandat, B., Adnet, S., Marivaux, L., Martinez, A., Vianey-Liaud, M., Tabuce, R., 2012. A  
1136 new mammalian fauna from the earliest Eocene (Ilerdian) of the Corbières (Southern  
1137 France): palaeobiogeographical implications. *Swiss Journal of Geosciences*, 105(3),  
1138 417–434.
- 1139 Missiaen, P., Quesnel, F., Dupuis, C., Storme, J.-Y. & Smith, T., 2013. The earliest Eocene  
1140 mammal fauna of the Erquelinnes Sand Member near the French-Belgian border.  
1141 *Geologica Belgica*, 16(4): 262-273.
- 1142 Nel, A., Ploeg G.D., Dejax, J., Dutheil, D., Fransceschi, D.D., Gheerbrant, E., Godinot, M.,  
1143 Hervet, S., Menier, J.-J., Augé, M., Bignot, G., Cavagnetto, C., Duffaud, S., Gaudant, J.,  
1144 Hua, S., Jossang, A., Lapparent de Broin, F.D., Pozzi, J.-P., Paicheler, J.-C., Beuchet,  
1145 F., Rage, J.-C., 1999. Un gisement sparnacien exceptionnel à plantes, arthropodes et  
1146 vertébrés (Eocène basal, MP7) : Le Quesnoy (Oise, France). *Comptes Rendus de*  
1147 *l'Académie des Sciences, Paris* 329: 65–72.
- 1148 Orliac, M.J., Ducrocq, S., 2012. Eocene raoellids (Mammalia, Cetartiodactyla) outside the  
1149 Indian Subcontinent: palaeogeographical implications. *Geological Magazine*, 149(01),  
1150 80–92.
- 1151 Orliac, M.J., Gilissen, E., 2012. Virtual endocranial cast of earliest Eocene *Diacodexis*  
1152 (Artiodactyla, Mammalia) and morphological diversity of early artiodactyl brains.  
1153 *Proceedings of the Royal Society of London B: Biological Sciences*, 279(1743), 3670–  
1154 3677.
- 1155 Orliac, M.J., O’Leary, M.A., 2014. Comparative anatomy of the petrosal bone of  
1156 dichobunoids, early members of Artiodactylamorpha (Mammalia). *Journal of*  
1157 *Mammalian Evolution*, 21(3), 299–320.
- 1158 Orliac, M. J., Karadenizli, L., Antoine, P. O., Sen, S., 2015. Small hyotheriine suids  
1159 (Mammalia, Artiodactyla) from the late Early Miocene of Turkey and a short overview  
1160 of Early Miocene small suoids in the Old World. *Palaeontologia Electronica*, 18(2), 1–  
1161 18.
- 1162 Orliac, M.J., Boivin, M., Tabuce, R., in press. A mandible of *Diacodexis* cf. *gigasei*  
1163 (Artiodactyla, Diacodexidae) from the early Eocene locality of Palette (Bouches-du-  
1164 Rhône, France). *MorphoMuseum*.
- 1165 Rana, R.S., Kumar, K., Escarguel, G., Sahni, A., Rose, K.D., Smith, T., Singh, H., Singh, L.,  
1166 2008. An ailuravine rodent from the lower Eocene Cambay Formation at Vastan,  
1167 western India, and its palaeobiogeographic implications. *Acta Palaeontologica Polonica*  
1168 53, 1–14.

- 1169 Robinet, C., Remy, J.A., Laurent, Y., Danilo, L., Lihoreau, F., 2015. A new genus of  
1170 Lophiodontidae (Perissodactyla, Mammalia) from the early Eocene of La Borie  
1171 (Southern France) and the origin of the genus *Lophiodon* Cuvier, 1822. *Geobios*, 48(1),  
1172 25–38.
- 1173 Romer, A.S., 1966. *Vertebrate paleontology*, 3<sup>rd</sup> ed. University of Chicago Press, Chicago.
- 1174 Rose, K.D., 1982. Skeleton of *Diacodexis* oldest Known artiodactyl. *Science*, 216(4546),  
1175 621–623.
- 1176 Rose, K.D., 1996. On the origin of the order Artiodactyla. *Proceedings of the National*  
1177 *Academy of Sciences*, 93(4), 1705–1709.
- 1178 Rose, K.D., 2006. *Archaic ungulates. The beginning of the age of mammal*. John Hopkins  
1179 university press, Baltimore.
- 1180 Rose, K.D., Chew, A.E., Dunn, R.H., Kraus, M.J., Fricke, H.C., Zack, S.P., 2012. Earliest  
1181 Eocene mammalian fauna from the Paleocene-Eocene thermal maximum at Sand Creek  
1182 divide, Southern Bighorn Basin, Wyoming. *University of Michigan, Papers in*  
1183 *Paleontology*, 36, 1–122.
- 1184 Rose, K.D., Rana, R.S., Sahni, A., Kumar, K., Singh, L., Smith, T., 2009. First tillodont from  
1185 India: Additional evidence for an early Eocene faunal connection between Europe and  
1186 India? *Acta Palaeontologica Polonica* 54, 351–355.
- 1187 Russell, D.E., Thewissen, J.G.M., Sigogneau-Russel, D., 1983. A new dichobunoid  
1188 artiodactyl (Mammalia) from the Eocene of North-West Pakistan – II Cranial osteology.  
1189 *Proceedings of the Koninklijke Nederlandse Akademie van Wetenschappen, Series B*,  
1190 3, 285–300.
- 1191 Sigogneau-Russell, D., Russell, D.E., 1983 A new dichobunoid artiodactyl (Mammalia) from  
1192 the Eocene of North-West Pakistan - III Reconstitution du moulage endocrânien.  
1193 *Proceedings of the Koninklijke Nederlandse Akademie van Wetenschappen, Series B*,  
1194 3, 319–330.
- 1195 Smith, T., Rana, R.S., Missiaen, P., Rose, K.D., Sahni, A., Singh, H., Singh, L., 2007. High  
1196 bat (Chiroptera) diversity in the early Eocene of India. *Naturwissenschaften* 94, 1003–  
1197 1009.
- 1198 Smith, T., Rose, K.D., Gingerich, P.D., 2006. Rapid Asia–Europe–North America geographic  
1199 dispersal of earliest Eocene primate *Teilhardina* during the Paleocene–Eocene thermal  
1200 maximum. *Proceedings of the National Academy of Sciences*, 103(30), 11223–11227.



- 1201 Smith, R., Smith, T., Sudre, J., 1996. *Diacodexis gigasei* n. sp., le plus ancien Artiodactyle  
1202 (Mammalia) belge, proche de la limite Paléocène-Eocène. Bulletin de l'Institut Royal  
1203 des Sciences Naturelles de Belgique, Sciences de la Terre, 66, 177–186.
- 1204 Solé, F., J., F., Laurent, Y., 2014. New proviverrines (Hyaenodontida) from the early Eocene  
1205 of Europe; phylogeny and ecological evolution of the Proviverrinae. Zoological Journal  
1206 of the Linnean Society 171, 878–917.
- 1207 Solé, F., Smith, T., Tabuce, R., Marandat, B., 2017. New dental elements of the oldest  
1208 proviverrine, *Parvagula palulae*, from the early Eocene of Southern France and their  
1209 support for a possible African origin of the Proviverrinae (Hyaenodonta, Mammalia).  
1210 Acta Palaeontologica Polonica 60, 527–538.
- 1211 Stefen, C., 1999. Evolution of enamel microstructure of archaic ungulates ("Condylarthra")  
1212 and comments on some other early Tertiary mammals. Paleobios, 19, 15–36.
- 1213 Sudre, J., Russell, D., Louis, P., Savage, D.E., 1983. Les Artiodactyles de l'Eocène inférieur  
1214 d'Europe. I. Bulletin du Muséum National d'Histoire Naturelle. Section C, Sciences de  
1215 la terre, paléontologie, géologie, minéralogie, 5(3), 281–333.
- 1216 Sudre, J., Erfurt, J., 1996. Les artiodactyles du gisement yprésien terminal de Prémontré  
1217 (Aisne, France). Palaeovertebrata, 25(2-4), 391–414.
- 1218 Tabuce, R., Delmer, C., Gheerbrant, E., 2007a. Evolution of the tooth enamel microstructure  
1219 in the earliest proboscideans (Mammalia). Zoological Journal of the Linnean Society,  
1220 149(4), 611–628.
- 1221 Tabuce, R., Marivaux, L., Adaci, M., Bensalah, M., Hartenberger, J.-L., Mahboubi, M.,  
1222 Mebrouk, F., Taffoeau, P., Jaeger, J.-J., 2007b. Early Tertiary mammals from North  
1223 Africa reinforce the molecular Afrotheria clade. Proceedings of the Royal Society B:  
1224 Biological Science, 274, 1159–1166.
- 1225 Tabuce, R., Seiffert, E.R., Gheerbrant, E., Alloing-Séguier, L., Koenigswald, W. von., 2017.  
1226 Tooth enamel microstructure of living and extinct hyracoids reveals unique enamel  
1227 types among mammals. Journal of Mammalian Evolution, 24, 91–110.
- 1228 Tabuce, R., Antunes, M.T., Smith, R., Smith, T., 2006. Dental and tarsal morphology of the  
1229 European Paleocene/Eocene "condylarth" mammal *Microhyus*. Acta Palaeontologica  
1230 Polonica 51, 37–52.
- 1231 Tabuce, R., Antunes, M.T., Sigé, B., 2009. A new primitive bat from the earliest Eocene of  
1232 Europe. Journal of Vertebrate Paleontology 29, 627–630.

- 1233 Tabuce, R., Clavel, J., Antunes, M.T., 2011. A structural intermediate between triisodontids  
1234 and mesonychians (Mammalia, Acreodi) from the earliest Eocene of Portugal.  
1235 *Naturwissenschaften* 98, 145–155.
- 1236 Tabuce, R., in press. — New remains of *Chambius kasserinensis* from the Eocene of Tunisia  
1237 and evaluation of proposed affinities for Macroscelidea (Mammalia, Afrotheria).  
1238 *Historical Biology*.
- 1239 Theodor, J.M., Erfurt, J., Métais, G., 2007. The earliest artiodactyls, in: Prothero, D.R., Foss,  
1240 S.E. (Eds). *The evolution of Artiodactyla*. Johns Hopkins university press, Baltimore,  
1241 pp. 32–58.
- 1242 Thewissen, J.G.M., Russell, D.E., Gingerich, P.D., Hussain, S.T., 1983. A new dichobunid  
1243 artiodactyl (Mammalia) from the Eocene of north-west Pakistan. *Proceedings of the*  
1244 *Koninklijke Nederlandse Akademie van Wetenschappen, Series B*, 86(2), 153–180.
- 1245 Van Valen, L.M., 1971. Toward the origin of artiodactyls. *Evolution*, 25(3), 523–529.
- 1246 Wible, J.R., Rougier, G.W., Novacek, M.J., Asher, R.J., 2009. The eutherian mammal  
1247 *Maelestes gobiensis* from the Late Cretaceous of Mongolia and the phylogeny of  
1248 Cretaceous Eutheria. *Bulletin of the American Museum of Natural History*, 327, 1–123.
- 1249 Yans, J., Marandat, B., Masure, E., Serra-Kiel, J., Schnyder, J., Storme, J.-Y., Marivaux, L.,  
1250 Adnet, S., Vianey-Liaud, M., Tabuce, R., 2014. Refined bio- (benthic foraminifera,  
1251 dinoflagellate cysts) and chemostratigraphy ( $\delta^{13}\text{C}_{\text{org}}$ ) of the earliest Eocene at Albas-  
1252 Le Clot (Corbières, France): implications for mammalian biochronology in Southern  
1253 Europe. *Newsletters on Stratigraphy* 47, 331–353.
- 1254 Zack, S.P., Penkrot, T.A., Krause, D.W., Maas, M.C., 2005. A new apheliscine 'condylarth'  
1255 mammal from the Late Paleocene of Montana and Alberta and the phylogeny  
1256 of 'hyopsodontids'. *Acta Palaeontologica Polonica*, 50(4), 809–830.
- 1257

1258 **Table and Figure captions**

<b>Tooth</b>	<b>Specimen</b>	<b>L</b>	<b>l</b>	<b>L/l</b>
<b>p</b>	UM SNC 386	2.83	1.05	2.71
<b>p</b>	UM SNC 64	2.91	0.93	3.13
<b>m1</b>	UM SNC 93	2.68	1.74	1.54
<b>m1</b>	UM SNC 6	2.65	1.89	1.40
<b>m1</b>	UM SV3-133	3.05	2.00	1.53
<b>m1</b>	UM SNC 74	2.72	1.76	1.55
<b>m2</b>	UM SNC 74	3.07	2.12	1.45
<b>m2</b>	UM SV3-338	3.43	2.14	1.60
<b>m2</b>	UM SNC 3	3.13	2.44	1.28
<b>m3</b>	UM SV3-129	4.27	2.59	1.65
<b>m3</b>	UM SV3-332	3.50	2.34	1.49
<b>m3</b>	UM SNC 63	3.51	2.02	1.74
<b>m3</b>	UM SNC 17	3.72	2.34	1.59
<b>m3</b>	UM SNC 65	3.71	2.24	1.66
<b>P3</b>	UM SNC 58	3.27	1.79	1.83
<b>P4</b>	UM SNC 33	2.43	2.97	0.82
<b>P4</b>	UM SNC 311	2.49	3.08	0.81
<b>P4</b>	UM SNC 405	2.32	3.38	0.69
<b>dP4</b>	UM SNC 13	3.15	3.24	0.97
<b>dP4</b>	UM SV3-131	2.91	2.58	1.13
<b>M1</b>	UM SNC 49	2.86	4.03	0.71
<b>M1</b>	UM SV3-163	2.72	3.45	0.79
<b>M1</b>	UM SV3-189	2.66	3.40	0.78
<b>M1</b>	UM SV3-128	2.97	3.70	0.80
<b>M1</b>	UM SNC 339	-	3.59 *	-
<b>M2</b>	UM SV3-74	3.07	4.11	0.75
<b>M2</b>	UM SNC 20	3.07	3.79	0.81
<b>M2</b>	UM SNC 25	2.98	3.79	0.79
<b>M2</b>	UM SNC 36	3.15	3.95	0.80
<b>M2</b>	UM SNC 55	3.27	4.11	0.80
<b>M2</b>	UM SNC 95	3.50	4.02	0.87
<b>M3</b>	UM SNC 18	2.38	3.20	0.74
<b>M3</b>	UM SNC 262	2.52	3.34	0.75
<b>M3</b>	UM SV3-126	3.16	3.65	0.87

1259

1260 **Table 1.** Dental measurements of the new material of *Diacodexis antunesi* from Silveirinha,

1261 Portugal described in this work. Abbreviations: L, maximal length; l, maximal width, \*

1262 corresponds to estimated value on broken material.

1263

Locality specimen	Silveirinha	Palette	Palette
	UM SNC 687	UM PAT 168	UM PAT 19
Length (L)	-	7.08	6.90
Width body (I1)	4.17	4.15	3.76
Width neck (I2)	2.31	2.62	2.57
Width head (I3)	-	3.68	3.68
Length head (L3)	-	2.33	2.05
Length sust. fac. (Ls)	2.85	3.57	3.54
Width sust. fac. (ls)	2.02	2.16	2.42
Width navic. fac. (ln)	-	2.44	2.37

1264

1265 **Table 2.** Measurements of the astragalus from the MP7 localities of Silveirinha and Palette.

1266

tooth	specimen	L	l	L/l
p	UM FDN 279	2.80	1.25	2.25
dp4	UM FDN 123	3.51	1.61	2.18
m1	UM FDN 255	3.19	2.312	1.38
m1	UM FDN 124	3.27	2.20	1.49
m2	UM FDN 125	3.57	2.88	1.20
P2	UM FDN 252	-	1.33	2.07
P3	UM FDN 251	3.30	2.34	1.41
P3	UM FDN 283	2.89	2.03	1.42
P4	UM FDN 283	2.39	2.75	0.87
M2	UM FDN 283	3.12	4.13	0.76
M3	UM FDN 283	2.82	3.71	0.76

1267

1268 **Table 3.** Dental measurements of *Diacodexis* aff. *antunesi* from Fordones, France. .

1269 Abbreviations: L, maximal length; l, maximal width.

1270

<b>tooth</b>	<b>specimen</b>	<b>L</b>	<b>l</b>	<b>L/l</b>
<b>m1-m3</b>	UM PAT 159	11.23	-	-
<b>p4-m3</b>	UM PAT 159	14.93	-	-
<b>p3-m3</b>	UM PAT 159	18.55	-	-
<b>c (alveolus)</b>	UM PAT 159	2.13	0.93	-
<b>p1 (alveolus)</b>	UM PAT 159	2.29	1.02	-
<b>p2 (alveolus)</b>	UM PAT 159	3.42	1.21	-
<b>p3</b>	UM PAT 159	3.74	1.60	2.34
<b>p4</b>	UM PAT 159	3.79	2.04	1.86
<b>m1</b>	UM PAT 159	3.02	2.43	1.25
<b>m1</b>	UM PAT 136	3.23	2.16	1.50
<b>m2</b>	UM PAT 159	3.58	2.96	1.21
<b>m3</b>	UM PAT 159	4.63	2.91	1.59

1271

1272 **Table 4.** Dental measurements of *Diacodexis* cf. *gigasei* from Palette, France. Abbreviations:

1273 L, maximal length; l, maximal width.

1274

<b>tooth</b>	<b>specimen</b>	<b>L</b>	<b>l</b>	<b>L/l</b>
<b>m1</b>	UM APSO.2015.SP2-302	4.20	2.83	1.48
<b>P3</b>	UM BRI1	3.30	2.40	1.37
<b>P4</b>	UM BRI2	2.76	3.04	0.91
<b>M2</b>	UM BRI3	3.69	-	-
<b>M3</b>	UM BRI4	2.67	4.08	0.65

1275

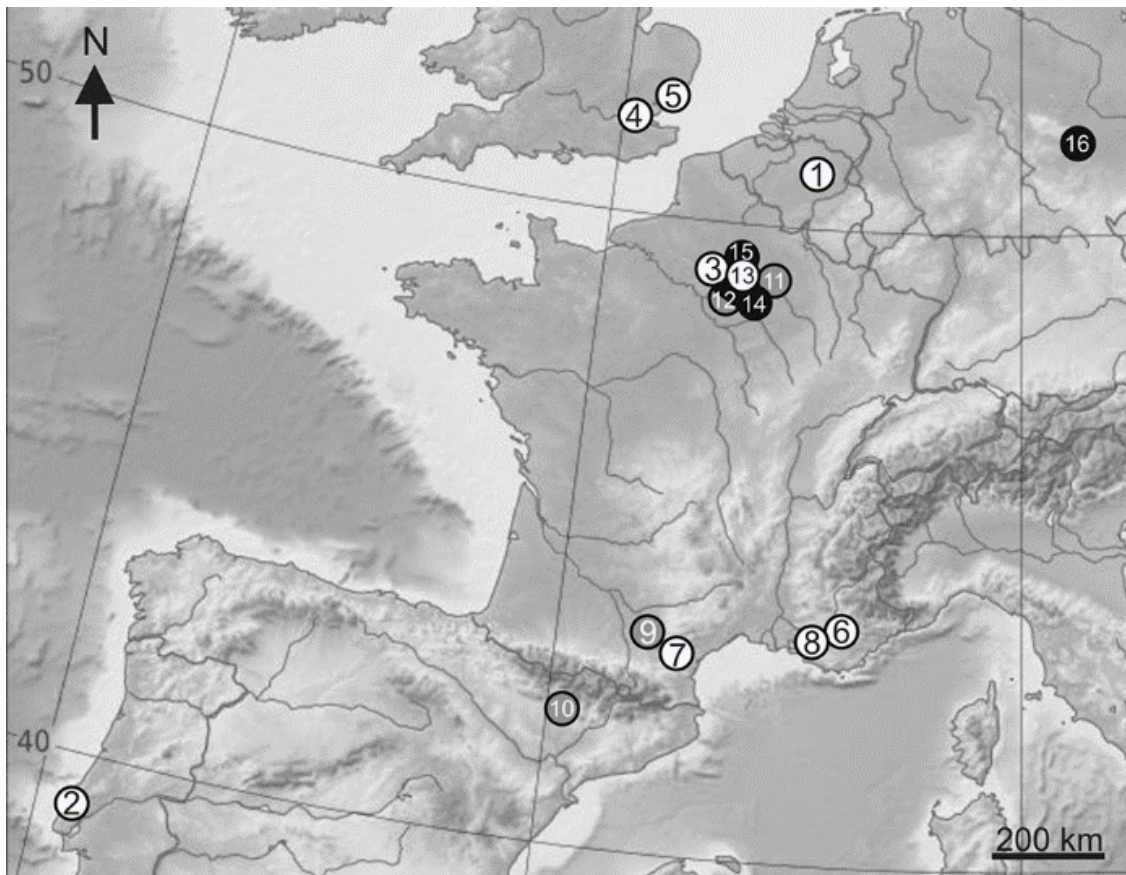
1276 **Table 5.** Dental measurements of *Diacodexis* sp. from La Borie, France. Abbreviations: L,

1277 maximal length; l, maximal width.

1278

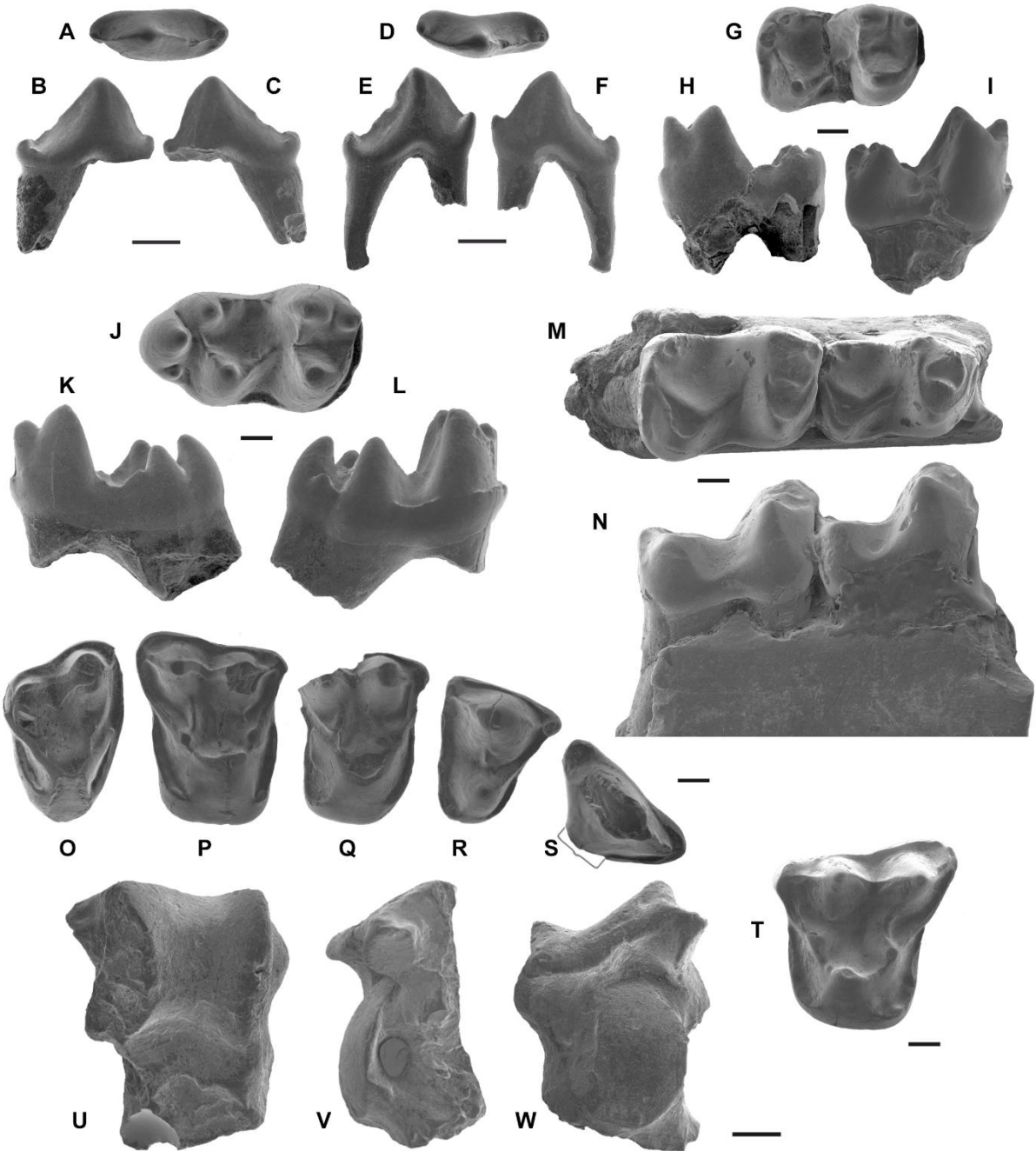
1279

1280



1281 **Figure 1.** Map showing early Eocene *Diacodexis*-bearing localities in Europe (MP7, MP8+9,  
1282 and MP10 localities are indicated by white, grey, and black circles, respectively): 1- Dormaal,  
1283 Belgium; 2-Silverinia, Portugal; 3-Le Quesnoy, France; 4- Abbey Wood, UK; 5-Kyson, UK;  
1284 6-Rians, France; 7-Fordones, France; 8- Palette, France; 9-La Borie, France; 10- Corsà 0,  
1285 Spain; 11-Avenay and Mutigny, France; 12-Condé-en-Brie and Saint-Agnan, France; 13-  
1286 Pourcy, France; 14-Grauves, Cuis, and Mancy, France; 15-Prémontré, France; 16- Geiseltal,  
1287 Germany.

1288

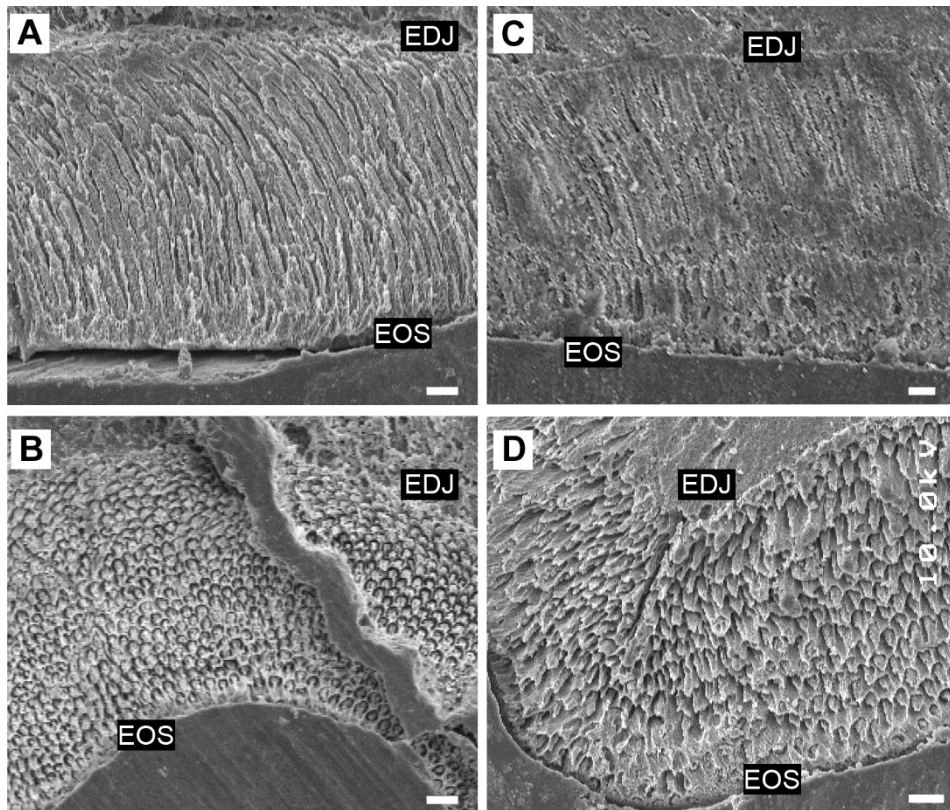


1289

1290 **Figure 2.** Dental and postcranial remains of *D. antunesi* from Silveirinha Pequena, Baixo  
 1291 Mondego, Portugal. A-C, SNC 64, p2/3?; D-F SNC 386, dp2/3?; G-I SNC 93, m1; J-L, SNC  
 1292 63, m3; M-N, SNC 74, m1-2; O, SNC 18, M3; P, SNC 20, M2; Q, SNC 339, M1; R, SNC  
 1293 311, P4; S, SNC 58, P3; T, SNC 13, dP4; U-W, SNC 687, astragalus. Views: A, D, G, J, M,  
 1294 O-T, occlusal; B, E, I, L, N, lingual; C, F, H, K, labial; U, anterior; V, lateral; W, posterior.  
 1295 Scale bars: A-F=1mm; G-T=0.5mm; U-W=1mm.

1296

1297



1298

**Figure 3.** Enamel microstructure in A-B, *D. antunesi* from Silveirinha Pequena, Baixo

1299

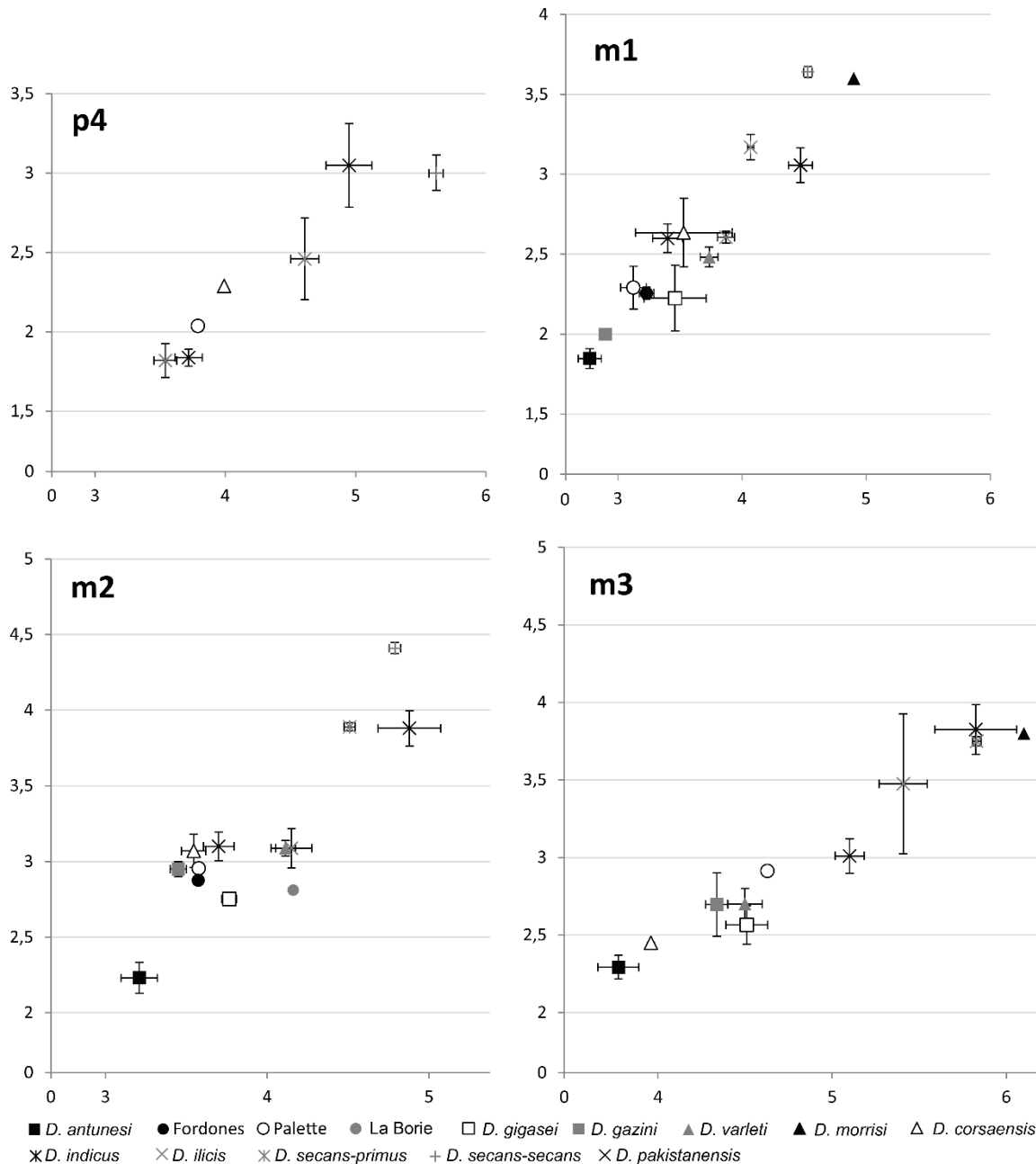
Mondego, Portugal and C-D, *D. aff. antunesi* from Fordones, Aude, France A-C horizontal

1300

plane, B-D tangential plane. Scale bar = 10µm.

1301





1302

1303

**Figure 4.** Biplots of lower dentition measurements with standard error. X=length, Y=width.

1304

Measurements from: *D. antunesi*, Estravis and Russell (1989) and Table 1; Fordonnes,

1305

Marandat (1991) and Table 3; Palette, Table 4; La Borie, Table 5; *D. gigasei*, Smith et al.

1306

(1996); *D. gazini*, Godinot (1981); *D. varleti*, Sudre et al. (1983); *D. morrisi*, Hooker (2010);

1307

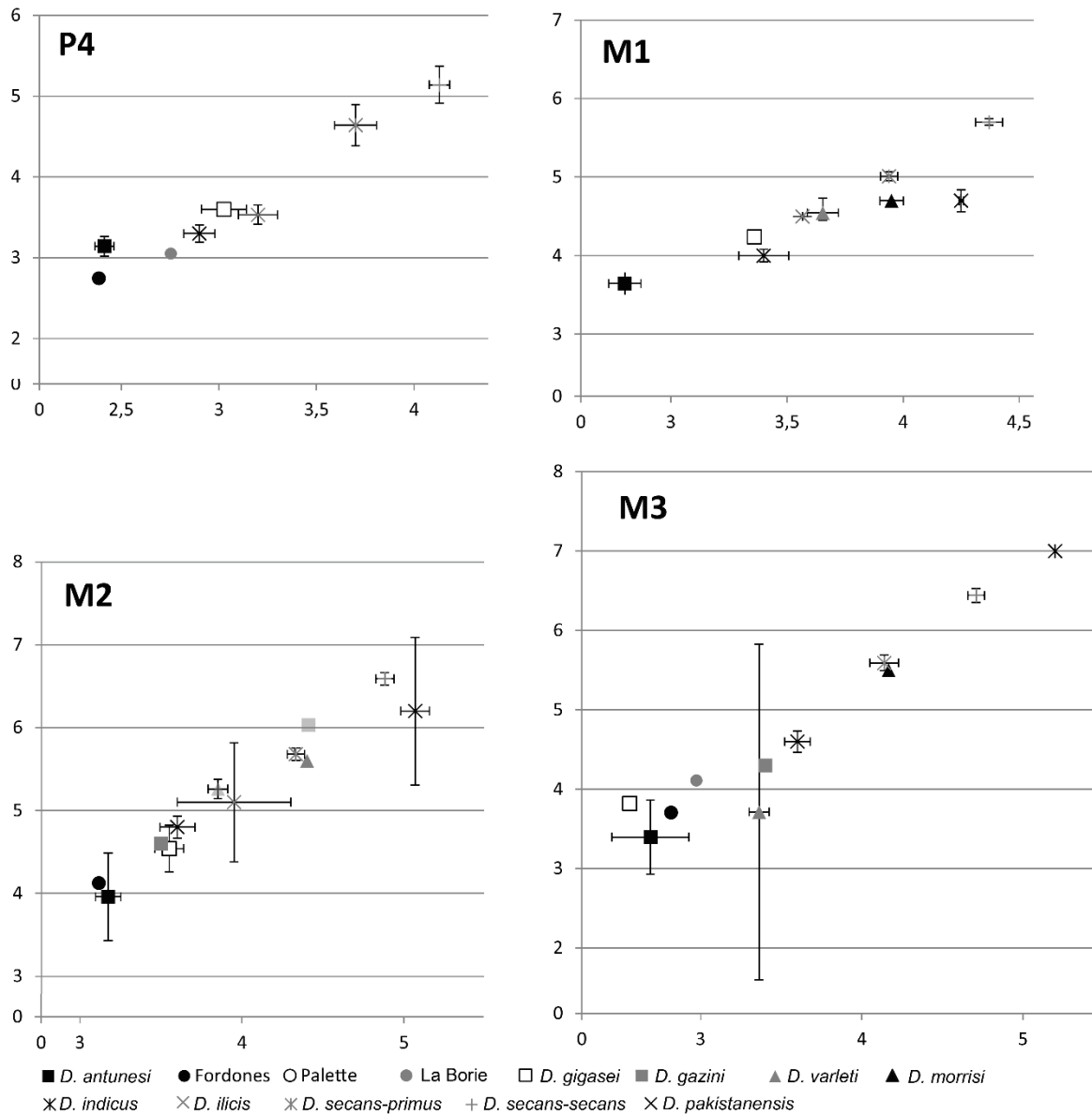
*D. corsaensis*, Checa Soler (2004); *D. indicus*, Kumar et al. (2010); *D. ilicis*, Gingerich

1308

(1989) and Rose et al. (2012); *D. secans primus*, Krishtalka and Stucky (1985); *D. secans*

1309

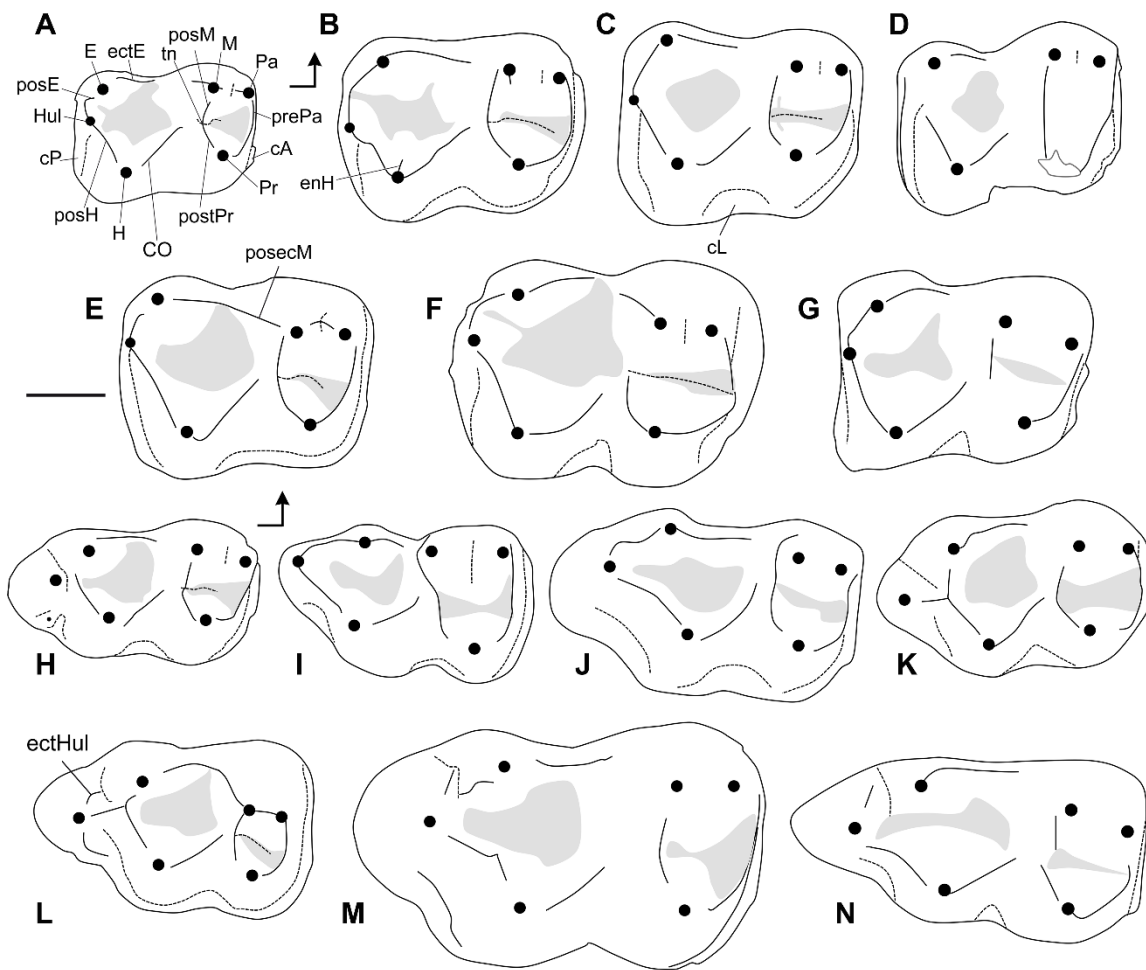
*secans*, Krishtalka and Stucky (1985); *D. pakistanensis*, Thewissen et al. (1983).



1310

1311 **Figure 5.** Biplots of upper dentition measurements with standard error. X=length, Y=width.  
 1312 Measurements from: *D. antunesi*, Estravis and Russell (1989) and Table 1; Fordonnes,  
 1313 Marandat (1991) and Table 3; Palette, Table 4; La Borie, Table 5; *D. gigasei*, Smith et al.  
 1314 (1996); *D. gazini*, Godinot (1981); *D. varleti*, Sudre et al. (1983); *D. morrisi*, Hooker (2010);  
 1315 *D. corsaensis*, Checa Soler (2004); *D. indicus*, Kumar et al. (2010); *D. ilicis*, Gingerich  
 1316 (1989) and Rose et al. (2012); *D. secans primus*, Krishtalka and Stucky (1985); *D. secans*  
 1317 *secans*, Krishtalka and Stucky (1985); *D. pakistanensis*, Thewissen et al. (1983).

1318



1319

1320 **Figure 6.** Lower dentition of *Diacodexis* species. A-G m2 of: A, *D. antunesi* SV3 338; B, *D.*

1321 *gigasei* IRScNB M 1815; C: *D. cf. gigasei* PAT 152; D: *D. aff. antunesi* FDN 125; E, *D.*

1322 *gazini* RI 163; F: *D. varleti* CB 1276, G: *D. pakistanensis* HGSP 300 5003. H-N, m3s: H, *D.*

1323 *antunesi* SNC 63; I, *D. gigasei* IRScNB M 116; J, *D. cf. gigasei* PAT 152; K, *D. varleti* CB

1324 579; L, *D. gazini* RI 162; M: *D. morrissi* M60060; N, *D. pakistanensis* HGSP 300 5003.

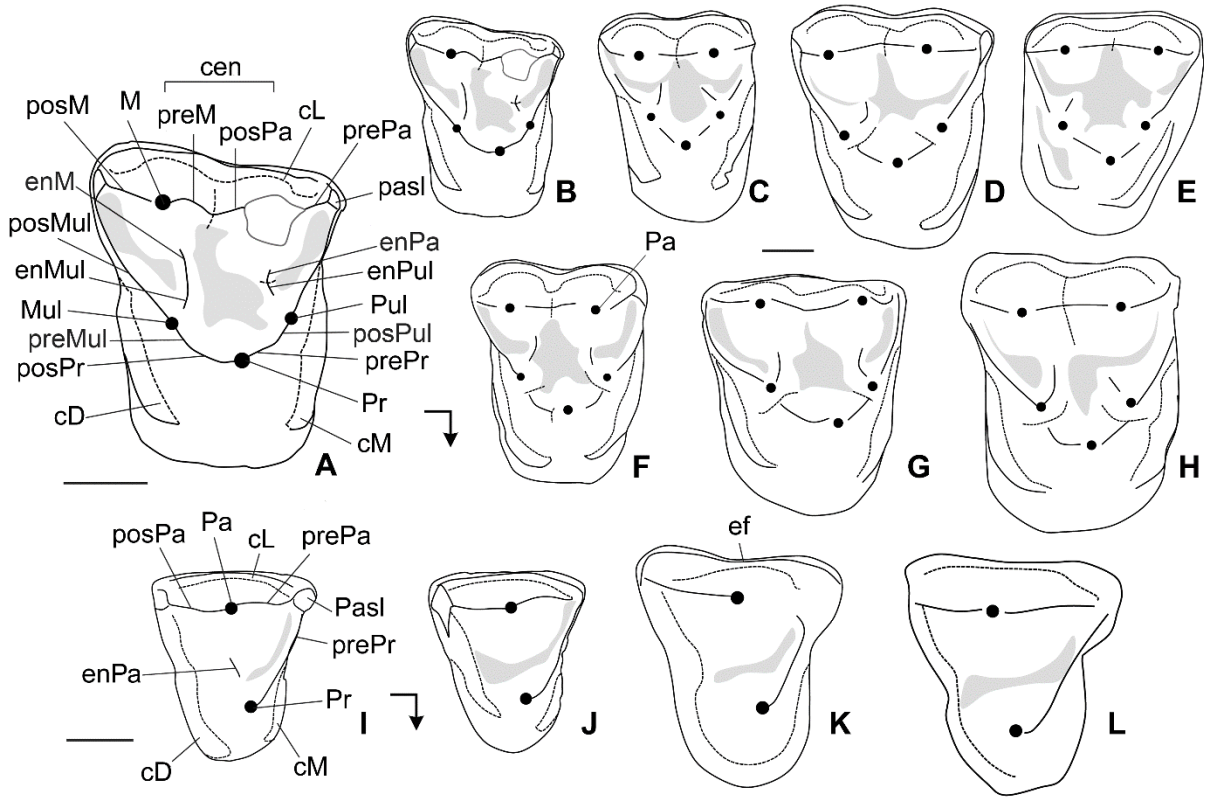
1325 Abbreviations: cP, posterior cingulid; cL, labial cingulid; cM, mesial cingulid; CO, cristid

1326 obliqua (= prehypocristid); ectE, ectoentocristid; ectHul, ectohypocristulid; enH,

1327 endohypocristid; E, entoconid; H, hypoconid; Hul, hypoconulid; M, metaconid; Pa,

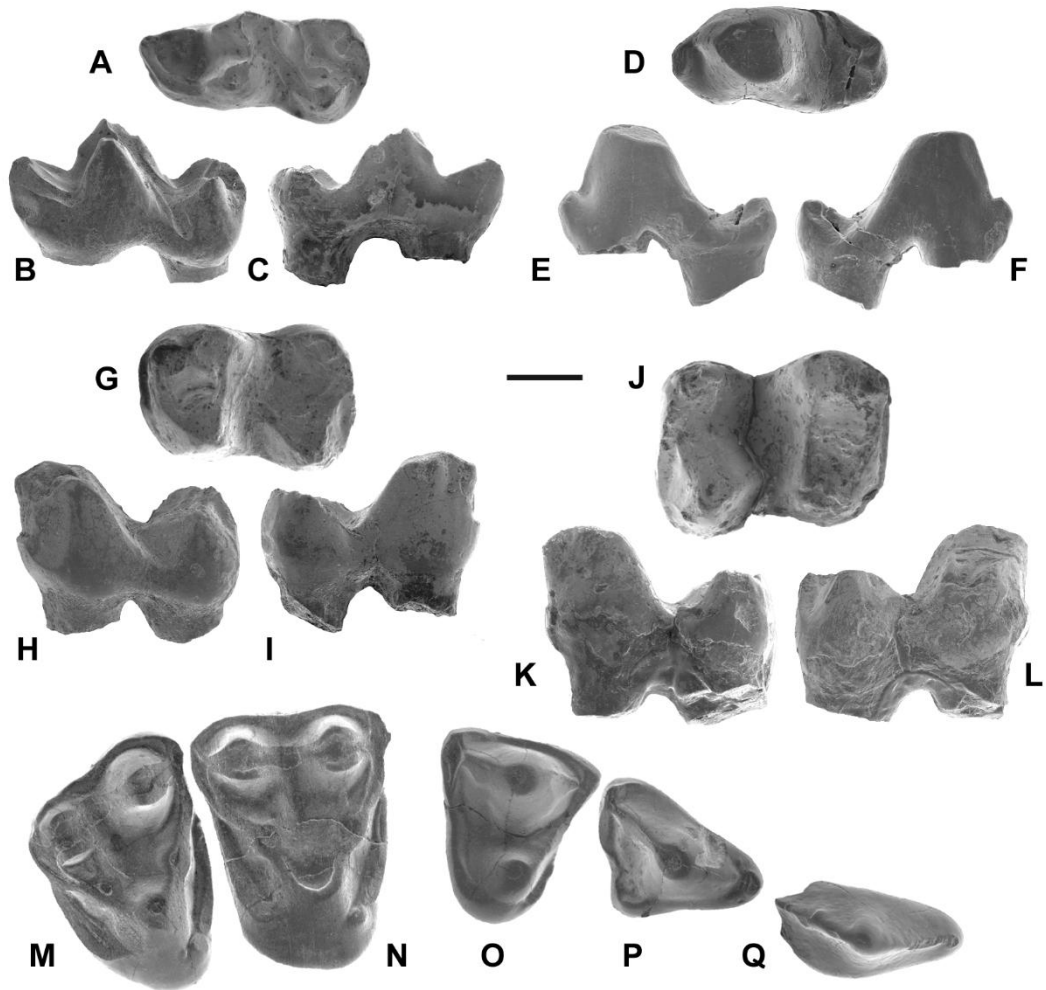
1328 paraconid; posecM, postectometacristid; posE, postentocristid; posH, posthypocristid; posM,

1329 postmetacristid; posPr, postprotocristid; prePa, preparacristid; Pr, protoconid; tn, trigonid  
 1330 notch. Modified after Kumar et al. (2010) and Orliac & Ducrocq (2011).



1331  
 1332 **Figure 7.** Upper dentition of *Diacodexis* species. A-H: M1 or M2 of: A-B, *D. antunesi* SNC  
 1333 20; C, *D. aff. antunesi* FDN 283; D, *D. varleti* CB 973; E, *D. gazini* RI 168; F, *D. gigasei*  
 1334 IRScNB M 1820; G, *D. morrissi* M44943; H, *D. ilicis* USNM 538412. I-L: P4 of: I, *D.*  
 1335 *antunesi* SNC 311; J, *D. aff. antunesi* FDN 283; K, *D. gigasei* IRScNB M1822; L, *D. ilicis*  
 1336 USNM 538412. Abbreviation: cen, centrocrista; cD, distal cingulum; cL, labial cingulum;  
 1337 cM, mesial cingulum; ef, ectoflexus; enMul, endometacristule; enPr, endoprotocrista; enPul,  
 1338 endoprotocristule; M, metacone; Mul, metaconule; enPul, endoparacristule; Pa, paracone;  
 1339 Pasl, parastyle; posPa, postparacrista; posM, postmetacrista; posMul, postmetacristule;  
 1340 posMuld, postmetacristule deflection; posPr, postprotocrista; prePa, preparacrista; prePr,  
 1341 preprotocrista; preM, premetacrista; prePr, preprotocrista; Pr, protocone; Pul, protoconule.  
 1342 Modified after Kumar et al. (2010) and Orliac & Ducrocq (2011).

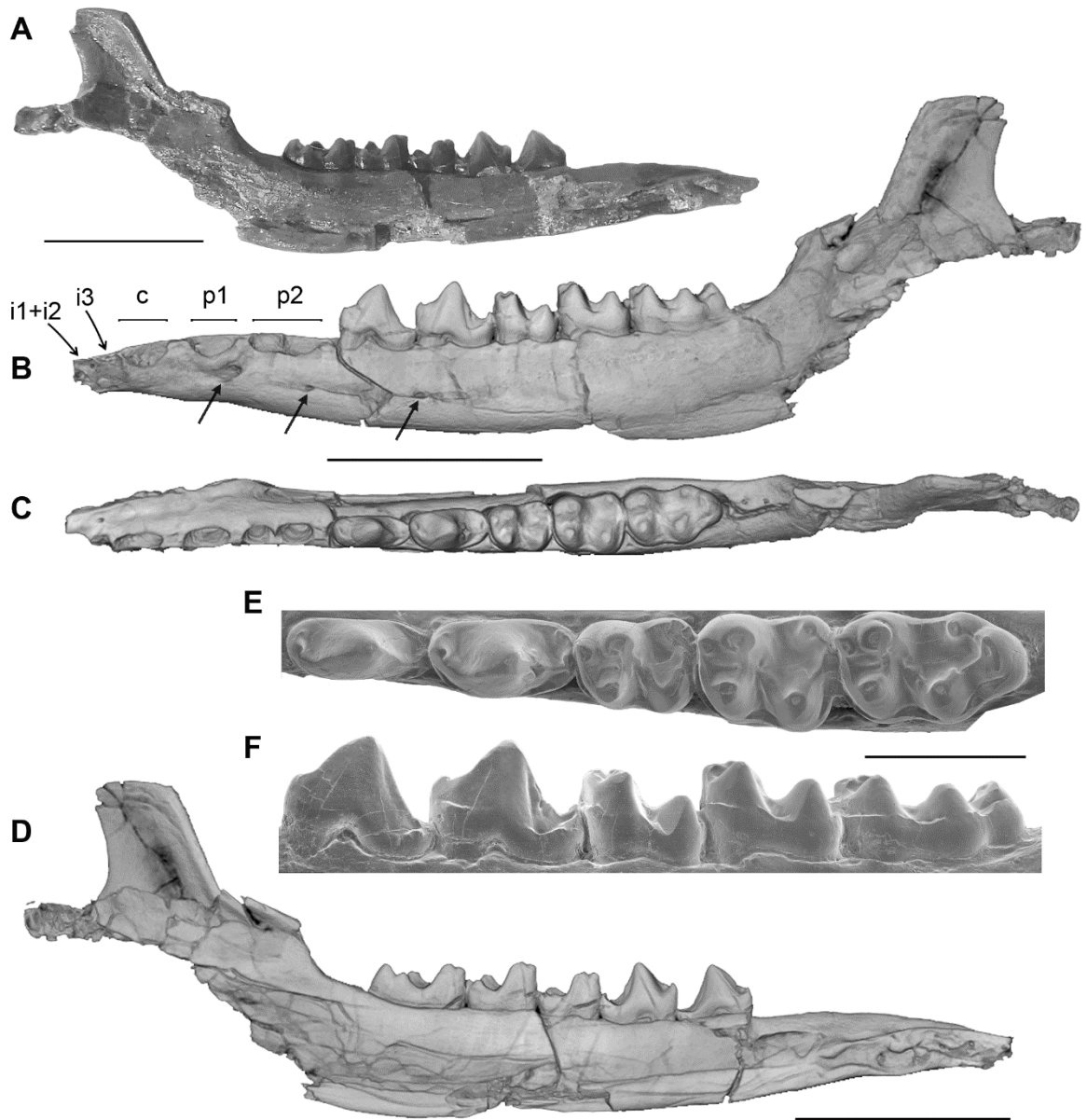
1343



1344

1345 **Figure 8.** Dental remains of *D. aff. antunesi* from Fordones, Aude, France. A-C, FDN 123,  
 1346 dp4; D-F, FDN 279, p2 or p3; G-I, FDN 124, m1; J-L, FDN 125, m2; M-P, associated upper  
 1347 tooth row, from right to left M3, M2, P4, P3 (FDN 283); Q, P2 (FDN 252). All material  
 1348 figured at the same scale. Views: A, D, G, J, M-Q, occlusal; B, F, H, L, labial; C, E, I, K,  
 1349 lingual. Scale bar=1mm.

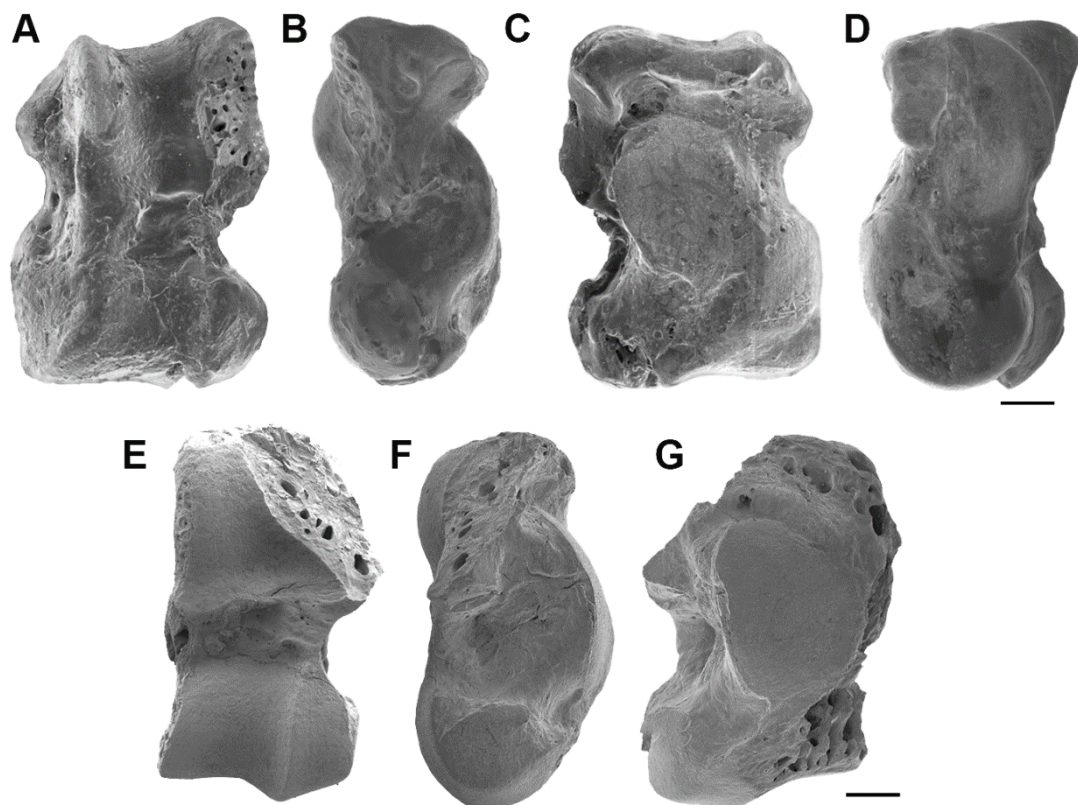
1350



1351

1352 **Figure 9.** *Diacodexis cf. gigasei* from Palette. A, PAT 159 medial view; B-D virtual 3D  
 1353 model of PAT 159 in B, medial, C, occlusal, D, lateral views; E-F, details of the teeth row in  
 1354 E, occlusal and F, labial view. Arrows indicate location of mental foramina. Scale bars = 1cm  
 1355 for A-D, 5 mm for E-F.

1356

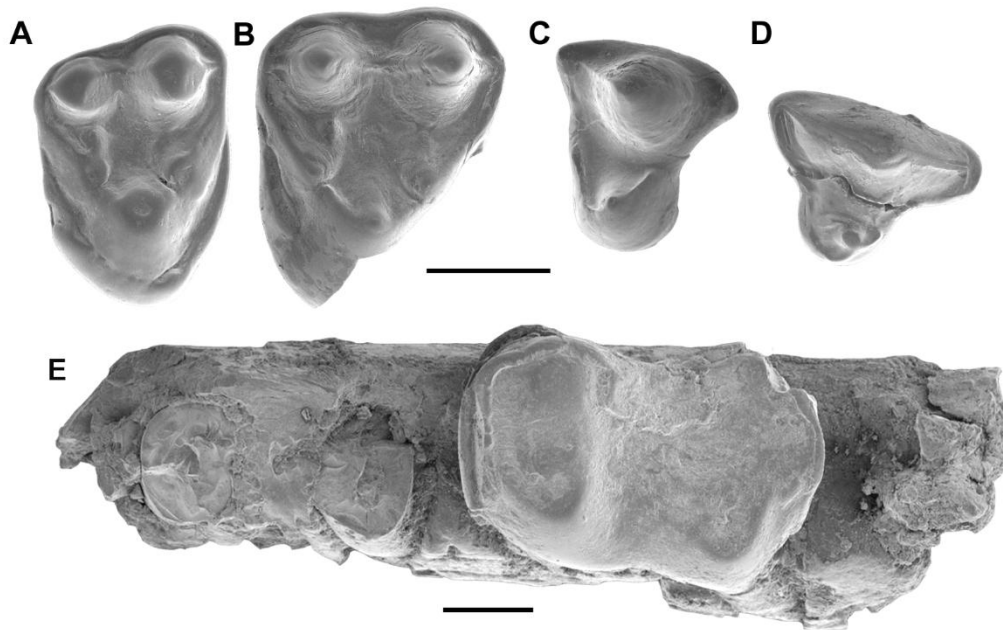


1357

1358 **Figure 10.** Astragali of *Diacodexis* cf. *gigasei* from Palette. A-D, left astragalus (PAT 19) in  
1359 A, anterior; B, lateral; C, posterior; D, medial views; E-G, right astragalus (PAT 168) mirror  
1360 view, in E, anterior; F, lateral; G, posterior views. Scale bars = 1 mm.

1361

1362



1363

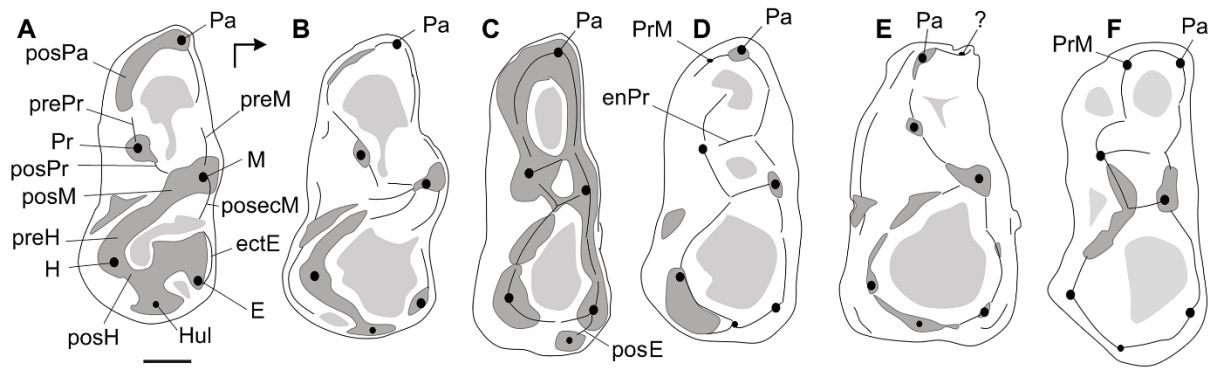
1364 **Figure 11.** Dental remains of *Diacodexis* sp. from La Borie, Aude, France. A, BRI 4, M3; B,

1365 BRI 3, M2; C, BRI 2, P4; D, BRI 1, P3 ; E, MHNT.PAL.2017.21.2, m2 on a fragmentary

1366 dentary. Scale bars: A-D = 1.5 mm ; E = 1 mm.

1367





1368

1369 **Figure 12.** Schematic pattern of grooves and crests of the lower fourth deciduous premolar of

1370 Diacodexeinae and Eurodexeinae. A, *D. aff. antunesi* (FDN 123); B, *D. morrisi* (M63703;

1371 drawn after Hooker 2010:fig.48E); C, *Diacodexis indicus* (Gu 513; drawn after Kumar et al.,

1372 2010); D, *Diacodexis* sp. from Prémontré (UM PRE151); E, *D. cf. varleti* from Prémontré

1373 (SLP-29-PE 637) mentioned by Sudre and Erfürt (1996); F, Eurodexeinae indet. from

1374 Prémontré (SLP 29PR 2122) according to Sudre and Erfürt (1996). Scale bar = 0.5 mm. Full

1375 lines originating from cuspids represent crests; dark grey surfaces represent worn surfaces;

1376 light grey surfaces represent basins. Abbreviations: ectE, ectoentocristid; E, entoconid; enPr,

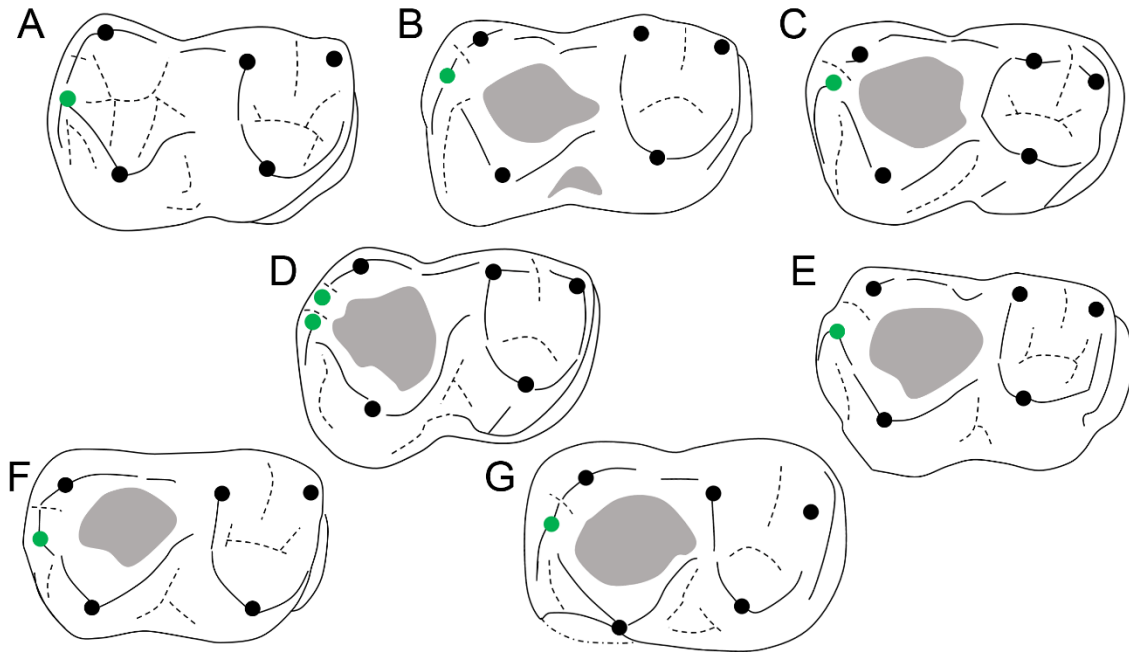
1377 endoprotocristid; H, hypoconid; Hul, hypoconulid; M, metaconid; Pa, paraconid; posecM,

1378 postectometacristid; posE, postentocristid; posH, posthypocristid; posM, postmetacristid;

1379 posPa, postparacristid; posPr, postprotocristid; preH, prehypocristid; preM, premetacristid;

1380 prePa, preparacristid; Pr, protoconid; prePr, preprotocristid; PrM, primonid.

1381



1382

1383 **Figure 13.** Schematic pattern of grooves and crests of the first lower molar in occlusal view  
 1384 of: A, *D. ilicis* (USNM 538371, after Rose et al., 2012: fig.51G); B, *D. antunesi* (SNC 63); C,  
 1385 *D. indicus* (GU 29, after Kumar et al., 2010: fig.7D, mirror view); D, *D. morrisi* (holotype,  
 1386 M83071, after Hooker, 2010: fig.47e), E, *D. varleti* (holotype, MNHN CB 255); F, *D. gigasei*  
 1387 (IRScNB M 1816, after Smith et al., 1996: pl. 1.2a); G, *D. gazini* (RI 165). Full lines  
 1388 originating from cuspids represent crests, dotted lines represent grooves, grey surfaces  
 1389 represent the basin of the talonid. The hypoconulid is highlighted in green. Not to scale.  
 1390